# 國 立 交 通 大 學

# 電機與控制工程學系

# 博士論文

禪坐中心血管系統及中樞神經系統電生
理現象之研究

Research on Cardiovascular System and
CNS Electrophysiological Phenomena
under Zen Meditation

研究生：劉權毅

指導教授：羅佩禎　博士

中華民國九十六年十二月

# 禪坐中心血管系統及中樞神經系統電生理現象之研究

# Research on Cardiovascular System and CNS
# Electrophysiological Phenomena under Zen Meditation

研 究 生：劉權毅　　　　　　　　　　Student：Chuan-Yi Liu

指導教授：羅佩禎　　　　　　　　　　Advisor：Pei-Chen Lo

國 立 交 通 大 學

電機與控制工程學系

博士論文

A Dissertation
Submitted to Department of Electrical and Control Engineering
College of Electrical and Computer Engineering
National Chiao Tung University
In Partial Fulfillment of the Requirements
For the Degree of
Doctor of Philosophy
in
Electrical and Control Engineering
December 2007
Hsinchu, Taiwan, Republic of China

中華民國九十六年十二月

獻給我的父母

劉正信先生與游燕墉女士

For My Dear Parents

Cheng-Hsin Liu and Yen-Yung Yu

# 禪坐中心血管系統及中樞神經系統電生理現象之研究

研 究 生：劉權毅　　　　　　　　　　指導教授：羅佩禎 博士

國立交通大學 電機與控制工程研究所

## 摘要

本篇論文在研究禪坐對於心血管系統，以及對於中樞神經系統的影響。在評估心血管系統的效應中，我們使用了血液壓力波的四種參數來量化禪坐對於血管系統的效果，這四種參數包括了 T 波的上昇斜率，以及 T 波、V3 波谷以及 D 波的正規化的高度。我們的實驗結果顯示，禪坐會加強心臟的搏出能力，得到較佳的動脈順應性，降低血管的阻塞，並強化動脈彈性以及主動脈瓣膜的功能。這些觀察結果可推論出禪坐的確可以促進心血管系統的相關特性。

禪坐者在禪坐過程中，常會體驗到有內在光芒的出現，為了研究此一普遍現象，我們設計了閃光視覺誘發電位實驗。在禪坐(放鬆)的前中後，我們對實驗組(控制組)受測者施以閃光刺激並蒐集視覺誘發電位。我們的實驗結果顯示在禪坐的過程中，後腦(Oz)位置上較晚的視覺誘發電位成分 N3-P3 以及 P3-N4，其振幅會較禪坐前降低，但是對於控制組(放鬆)而言，這些成分的振幅卻是增大的。此外，這些成分在中腦與前腦的振幅，在禪坐過程中是增加的，在休息中則是減少的。而某些成分的潛時(latency)在休息中是延長的，而禪坐中則是沒有太大的變化(P2 則有變化)。根據我們的發現，禪坐過程對於視覺神經系統以及大腦皮

質層的特定效應，和單純閉眼休息造成的效果是不一樣的。

在第四章中，我們探討了禪坐腦電波對於 alpha 波的空間聚集效果，並有了初步的結果。我們分別對於實驗組(禪坐)與控制組(閉眼放鬆)錄製腦電波，並使用小波分析方法對多頻道腦電波進行萃取 alpha 波的工作。我們再對正規化的 alpha 能量向量使用模糊分類演算法進行分類，以探討不同的空間分佈特性。分類過程中，我們對各群中心的模糊關係值向量進行相似度比對，以找出最佳的分類數。我們的結果顯示，前腦 alpha 活動發生的機率與禪坐的階段有關。從結果中可證實，禪坐過程中會產生三種空間-時間變化的分佈類型，而這是由於禪坐過程中的三個階段所產生的。此外，這兩組的後腦 alpha 活動也有不同的趨勢，控制組在禪坐過程中，後腦 alpha 的能量隨著時間呈現遞減的現象，但是實驗組則的後腦 alpha 一直呈現低於平常準位的現象。這些研究結果顯示，禪坐的過程大致上會分成三個階段，而各個階段對於 alpha 調變的機制有所差異。

在第三與第四章中，我們觀察到禪坐過程中，前額 alpha 有增加的趨勢，且視覺誘發電位與閉眼休息的情形下，也有不一樣的變化；因此我們設計了一種新的實驗，使受測者在相同的背景腦電波的條件—前額出現由 alpha 波主導的情況下，我們才對受測者施予閃光刺激。我們觀察了實驗組(禪坐者)與控制組(一般未練習禪坐者)兩者之間視覺誘發電位的差異，結果顯示，在禪坐中時，Cz 及 Fz 的位置上 P1-N2 and N2-P2 成分的振幅明顯增大，而控制組在休息時這些成份則會降低。因此，我們推測禪坐對於主要視覺皮質層及相關區域會有特定作用。

# Research on Cardiovascular System and CNS Electrophysiological Phenomena under Zen Meditation

Student：Chuan-Yi Liu                    Advisor：Dr. Pei-Chen Lo

Institute of Electrical and Control Engineering

National Chiao Tung University

## Abstract

This dissertation reports the effects of Zen meditation on cardiovascular system and CNS electrophysiological behaviors. In the aspect of cardiovascular study, we evaluated the effects of meditation on cardiovascular system based on four parameters derived from blood pressure wave (BPW) that included the rising slope, normalized height of T wave, normalized height of $V_3$ valley, and normalized height of D wave. The results showed that Zen meditation could lead to better heart ejection ability and aorta compliance, better arterial elasticity and aortic valve function, as well as the decreasing peripheral resistance of blood vessels. The observation allows us to infer that Zen meditation effectively improves functional characteristics of the cardiovascular system.

To investigate the common experience of meditation practitioners - perception of inner light during meditation, we designed the flash visual evoked potentials (F-VEPs) experiments. Flash stimuli were applied before, during and after meditation- / relaxation-session in experimental / control subjects. Our results show that amplitudes of late latency components N3-P3 and P3-N4 at Oz decrease during meditation in the

experimental group, whereas they increase in the control group. Both Cz and Fz amplitudes increase during meditation, yet decrease during relaxation for the control group. The latencies of some components increase under relaxation in control group, yet little variation (except P2) is observed in the meditators. According to our findings, Zen meditation induces particular effects on the visual nervous system and cortex that are distinguishable from those observed for normal relaxation.

In chapter 4, we report our preliminary results of investigating the spatial focalization of Zen-meditation EEG (electroencephalograph) in alpha band (8-13 Hz). For comparison, the study involved two groups of subjects, practitioners (experimental group) and non-practitioners (control group). Wavelet analysis was applied to multi-channel EEG signals to extract the alpha rhythm. Normalized alpha-power vectors were classified by Fuzzy C-means based algorithm to explore various brain spatial characteristics. Number of clusters was determined by correlation coefficients of the membership-value vectors of each cluster center. Our results show that, in the experimental group, the incidence of frontal alpha activity varies in accordance with the meditation stage. And the results demonstrated three different spatiotemporal modules consisting with three distinctive meditation stages normally recognized by meditation practitioners. The parietal alpha activity in two groups decreased in different ways. Particularly, monotonic decline was observed in the control group. The phenomenon might imply various mechanisms employed by meditation and relaxation in modulating parietal alpha.

In the research of visual perception under meditation based on alpha-dependent F-VEPs, we designed a strategy to record the F-VEPs under the consistent condition of background EEG – the emergence of dominant frontal alpha activity. According our preliminary results, the frontal alpha rhythms were more active during meditation. This event was thus used as the reference of meditation stage to trigger the flash stimuli. Based on the experimental protocol proposed, considerable differences between experimental and control groups were observed. In sum, amplitudes of P1-N2 and N2-P2 on Cz and Fz increased significantly during meditation, contrary to

the F-VEPs of control group at rest. We thus suggest that Zen meditation results in

acute response on primary visual cortex and the associated parts.

# 誌　謝

這段追求真理的時光，是我最快樂、最重要的歲月。

首先感謝指導教授羅佩禎老師，這幾年老師不只在專業領域上盡心盡力的教導，更在人生真理上給予我們更高更遠的視野；感謝老師始終秉持原則不斷挑剔、鞭策、引導我們，在這條孤獨的研究道路上，給予我信心與勇氣繼續往下走。

感謝口試委員楊谷洋、邱俊誠、謝仁俊、張剛鳴老師，老師們對於論文的不吝指導，讓我在論文研究上獲益匪淺。

感謝實驗室的學長姐：清泉、政勳、瑄詠，你們的指導與經驗，指引了我的研究方向，也導正了我許多的迷惘與疑惑。

特別感謝憲正與適達兩位同學，有你們兩位的互相砥礪，互相打氣，互相扶持，我才能在這條路上走下去；能有緣在這段時光與你們同行，是我最大的福氣；雖然往後大家各奔東西，但我會一直記得你們坐在我身旁，一起努力的景象。

感謝這幾年不斷麻煩我，騷擾我，幫助我的各位學弟：小波波、進忠、啟宏、仁隆、維廷、哲賢、槍哥、強哥、清文、政恩、昶毅、恩榮、敬達、小胖胖、Bono、宏彥，有你們的歡樂與活力，讓我的博班生活充滿了歡笑與光彩。

感謝室友阿昌這幾年來與我互相哈拉，也感謝他教我這麼多攝影的知識技術，雖然有很多我聽不懂。

感謝當初碩班的同學焦仕揚、威助、治亨，雖然只短短同學兩年，但是對我往後博班的影響與助益卻相當深遠。

最重要的是，感謝我的父母及兄姐，有你們的支持，我才能毫無後顧的投入這條研究的道路，才有可能完成這個人生的夢想；謝謝你們無怨無悔的付出，我永遠愛你們。

感謝大家的愛與支持，給予我源源不斷的溫暖，謝謝大家！

# Contents

# List of Tables

# List of Figures

# Chapter 1

# Introduction

Due to the therapeutic effectiveness, the new area *CAM* (*complementary and alternative medicine*) has drawn the attention of researchers and medical professionals in the past decades. Researches in biomedical engineering and life sciences should lay more stress on promoting the human health, in both the physiological and mental aspects. As a matter of fact, scientists of the West have been reporting substantial findings of the effectiveness of meditation practice in CAM not only on improving the physiological and mental health but on treating a number of diseases. Accordingly, our research laboratory (Biomedical Signal Research Lab) has been devoted to the study of Zen-Buddhist meditation since 1998. We investigate, from the viewpoint of biomedical engineering, phenomena of the human life system under the orthodox Zen meditation practice. We study the time-varying characteristics and dynamic mechanism during meditation course in order to further establish the correlation among different electrophysiological signals and parameters.

Meditation, classified as the category of *mind-body intervention* in complementary and alternative medicine (CAM), has been widely practiced on a daily basis for maintaining good health. To know more about its benefit to our body, a lot of

researches have been devoted to the study of meditation process and phenomena, mostly in the physiological and psychological aspects. Among various meditation techniques, we focus on Zen meditation that has been becoming popular during the past decades.

Since 1998, we have been investigating the Zen-meditation electroencephalography (EEG) and other physiological parameters in multi-faceted views, and abundant data and results have been accumulated and reported. This dissertation is mainly devoted to the study of Zen-meditation effects on cardiovascular system and brain electrophysiological behaviors based on the observation of blood pressure wave (BPW), EEG and flash evoked potentials (F-VEP).
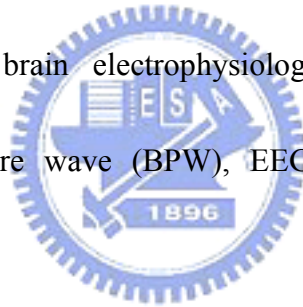
## 1.1 Background

Scientific exploration has corroborated the effectiveness of meditation practice on the health promotion which includes regulation of the hormone-level and blood pressure, moderation of stress and anxiety, reduction of chronic pain, etc (Dillbeck and Orme-Johnson, 1987; Jones, 2001; Walton et al., 1995; Barnes et al., 2001; Lindberg, 2005; Shetty, 2005). According to the experienced practitioners, meditation facilitates a greater sense of calmness, empathy, and compassion. As Western medical practitioners begin to understand the role of mind in health and disease, there has been more interest in both employing meditation in medicine and exploring brain dynamical phenomena during meditation. Electroencephalogram (EEG) thus becomes an important tool to monitor the meditation process (Niedermeyer and Lopez da Silva, 1999).
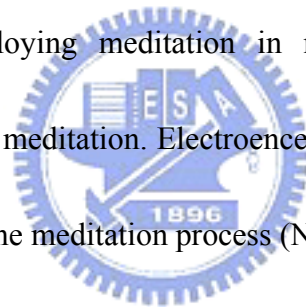
A thorough review of researches on meditation EEG can be found in (Cahn and Polich, 2006). Although much research has been devoted to investigating the physiological effects of meditation, many phenomena still have not yet been completely understood by people in CAM or in mainstream West medicine. According to our long-term interactions with the experienced practitioners for several years, the Zen meditation process involves experience of transcending various physiological, mental, and conscious states as follows. A meditation practitioner

would first attenuate their physical and mental sensors via particular mind-focusing technique, leave off the message transmission from outside world, and keep subconsciousness tranquil during meditation. Moreover, meditation practitioners often experience unusual perceptions, for example, loss or distortion of space and time perceptions, sensation of aureola-surroundings, etc. Especially, in the deeper meditation state, many meditation practitioners have experienced the *perception* of inner light (Lo et al., 2003). However, quite few studies were focused on this unique phenomenon reported by meditation practitioners. Accordingly, we aimed to investigate meditation effects on the visual neuronal pathway by quantifying the flash visual evoked potentials (F-VEPs). Furthermore, we investigated the relation between F-VEPs and frontal alpha waves often observed during meditation.
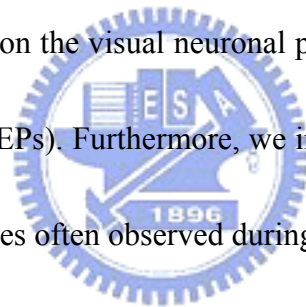
In addition, most studies about meditation effects on cardiovascular system emphasize the variation of blood-pressure range or electrocardiogram (ECG) signal, but few on the BPW (blood pressure wave) characteristics. Having been widely adopted in traditional Chinese medicine, BPW provides a more pronounced medium for characterizing Zen-meditation phenomena based on the concept of Qi-energy. This dissertation also presents a quantitative approach for investigating the variation of BPW patterns between the pre-meditation and post-meditation sessions.

## 1.2 Aim of this work

The main aim of this dissertation is to investigate the effects of Zen meditation on the cardiovascular system and brain electrophysiological behaviors. To attain this aim, we designed and carried out four experiments, for each presumed meditation phenomenon, to probe and further validate the results.

A number of literatures have reported the meditation effects on cardiovascular system. In particular, better control of blood pressure and modulation of heart rate variation (HRV) have drawn considerable attention of researchers (Barnes et al., 2004). They demonstrated that meditation might lower the blood pressure and therefore benefit people suffering from hypertension. To the best of our knowledge, the mechanisms digging into cardiovascular system behaviors have not been discussed.

In recent years, blood pressure wave, reflecting the meridian energy in TCB (traditional Chinese medicine) for thousand years, has been also employed in clinical diagnosis in conventional West medicine. The parameters of BPW have been used to investigate the characteristics of blood vessels of cardiac patients and normal subjects (Fey, 2003). Our previous study on HRV under Zen meditation revealed an apparent benefit to ANS (autonomous nervous system) and, hypothetically, to the cardiovascular system as well. We thus developed the strategy to study the effects of

meditation on cardiovascular system based on BPW analysis.

During the past decades, numerous researches about meditation EEG have been reported (Cahn and Polich, 2006). A few of them dealt with the characteristics of evoked potentials affected by meditation. Evoked potentials are the responses of central nervous system (CNS) to the external stimuli, including sounds (brainstem auditory evoked potentials, BAEP), light or pattern variations (visual evoked potentials, VEP), or electrical stimulation of peripheral nerves (somatosensory evoked potentials, SSEP). Each unique evoked potential characterizes the neuronal pathway corresponding to the control of particular sensory organ. According to the narration of Zen-meditation practitioners in our experiments, *inner-light* perception (Lo et al., 2003) is one of the common experiences in this group of subjects. This prompted us to study the meditation effects on visual neural pathway based on quantitative analysis of visual evoked potentials.

According to the researches of meditation EEG, variation of frontal alpha has been identified to be an exclusive brain electrophysiological phenomenon during or after the meditation course. In our study, the meditation session lasted 30 minutes or more. Note that EEG is non-stationary at the level of second. We developed a scheme, based on wavelet theory and fuzzy c-means, to investigate the spatial-temporal distribution of alpha power.

From the F-VEPs and spatiotemporal alpha studies described above, we noticed the issue of F-VEP variations due to background EEG. To make the experiment more conscientious, we proposed a hypothesis that F-VEP should be conducted under the same background EEG. As a consequence, a real-time alpha detection scheme was required. In this study, we collected F-VEPs upon the event that alpha wave presented on the frontocentral site (Fz).

## 1.3 Organization of the dissertation

This dissertation is composed of six chapters. In chapter 1, we introduce the background and the aim of our research. In addition, motivation and background of designing four studies are described. Chapter 2 reports the results and our findings of BPW research. The beginning of this chapter is devoted to the BPW mechanism, the experimental setup, and the signal processing method. The results and statistical analysis are presented at the end of the chapter.

Chapter 3 is focused on the F-VEP study. The first part includes the review of researches related to our work and the motivation of conducting this study. Illustration of experimental procedure follows. Finally the inter-session and inter-group comparisons are conducted.

In chapter 4, we proposed a method to monitor the spatio-temporal distribution of alpha waves using wavelet and fuzzy c-means. Finally, inter-group difference is justified by statistical analysis.

Chapter 5 describes the scheme for real-time alpha-rhythm detection employed in the F-VEP study. This study was attempted to explore the meditation effects on visual perception.

The last chapter summarizes the findings of four studies, that is, BPW, F-VEPs, spatiotemporal alpha, and alpha-dependent F-VEPs. This chapter concludes with our

anticipation of future work.

# Chapter 2

# Variation analysis of sphygmogram to assess the cardiovascular system under Zen meditation

In this chapter, we studied how meditation affects the characteristics of cardiovascular system, mainly based on the blood pressure waveform (BPW). Four parameters derived from the BPW include the rising slope ($\frac{h_1}{t_1}$), normalized height of T wave ($\frac{h_3}{h_1}$), normalized height of $V_3$ valley ($\frac{h_4}{h_1}$), and normalized height of D wave ($\frac{h_5}{h_1}$), where $t_1$ and $h_i$, $i = 1, \ldots, 5$ are quantitative features of the BPW waveform pattern.

## 2.1 Background and motivation

The blood pressure waveform (BPW) of the systemic arterial tree is an important determinative of cardiovascular system performance. This signal originates in the

systole and diastole of the heart and conveys such information as the blood ejection ability of the heart, the elasticity of the artery wall, the peripheral resistance, etc. (Milnor, 1989). In examinations of the clinical value of BPW, Han explored (Han, 2000) possible biophysical and pathological mechanisms of BPW from the viewpoint of hemodynamics. Research showed that BPW analysis is a highly reproducible method and easy to apply to clinical studies. This measure provides important information about arterial stiffness and cardio-vascular interactions (Wilkinson, 1998; O'Rourke1, 2001). Abnormality in the blood pressure waveform is linked to various physiological or pathological states such as aging and hypertension (Cohn et al., 1995; Mcveigh et al., 1999). Actually, the blood pressure waveform of radial artery detected at the wrist is the sphygmographical signal used in Traditional Chinese Medicine (TCM) (Tan, 2004). According to theory of the sphygmographical signal, the TCM clinician can identify the status of the human body and treat the patient.
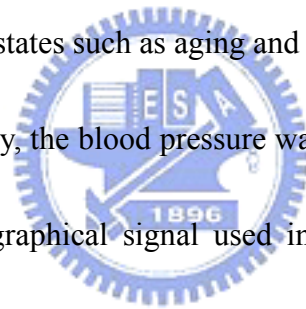
As more clinical evidence supported the benefits of meditation for health, about fifty years ago researchers began investigating the physiological phenomena of the human body under meditation. Dillbeck et al. (1987) compared the physiological differences in two groups of subjects, one under transcendental meditation and the other at rest. Schneider et al. (1995) found that the training of transcendental meditation could significantly lower the systolic and diastolic blood pressure of

hypertensive persons (Barnes et al., 2004; Alexander et al., 1996; Castillo-Richmond et al., 2000). Meditation hereafter became a feasible method to improve the hypertension. Hankey compared Tibetan Buddhist meditation with Transcendental Meditation (Hankey, 2006). He summarized how practicing different meditation techniques influenced hypertension and other physiological changes. Barnes et al. (1999) found that, under meditation, total peripheral resistance decreased, and they suggested that was why meditation could decrease or control hypertension. To investigate the meditation effects on the cardiovascular system, here we evaluated the variations in blood pressure waveform before and after meditation.

We measured the blood pressure waveforms of twenty Zen-meditation practitioners and twenty normal, healthy subjects in the same age range as the practitioners. According to the clinical experience of TCM professionals, we designed a set of parameters that quantify the waveform patterns of BPW.

## 2.2 Methods for BPW analysis

### 2.2.1 Mechanism and recording procedure

The BPW prototype of a healthy subject is shown in Fig. 2-1. The heart pumping mechanism correlating with BPW is illustrated as follows (see Fig. 2-2). The ejection of blood from the left ventricle into the aorta results in the first peak in BPW that is

called the Percussion wave (P wave). The height of P wave, $h_1$, and the fast ejection time of the left ventricle, $t_1$, are related to the ejection ability of heart and the compliance index of aorta. We define the rising slope of P wave as $\dfrac{h_1}{t_1}$. A larger slope indicates a better performance of the heart ejection function and aorta compliance (Fey, 2003). Thus it is used as a quantitative feature to evaluate the cardiovascular system.
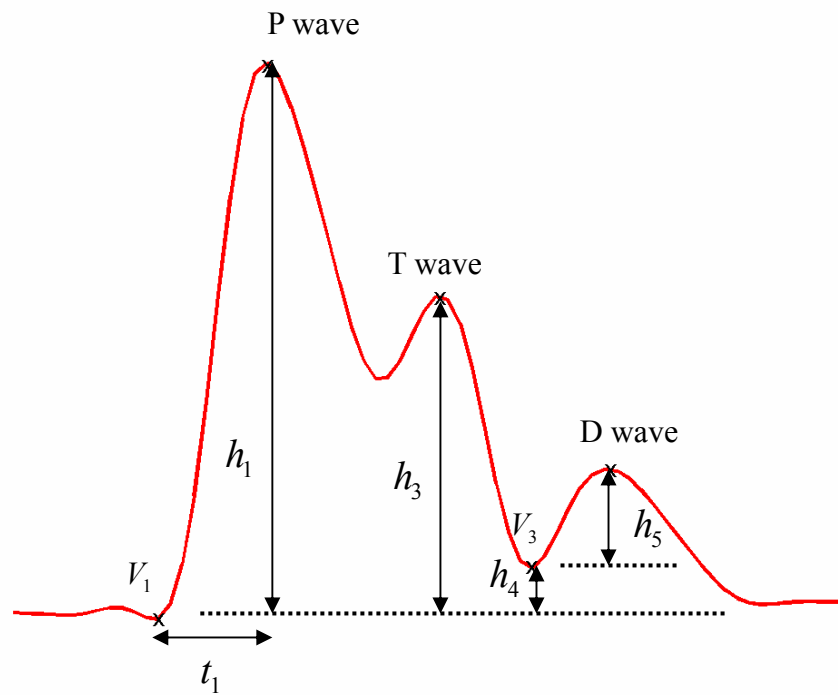


Figure 2-1: Prototype of a normal blood pressure waveform.
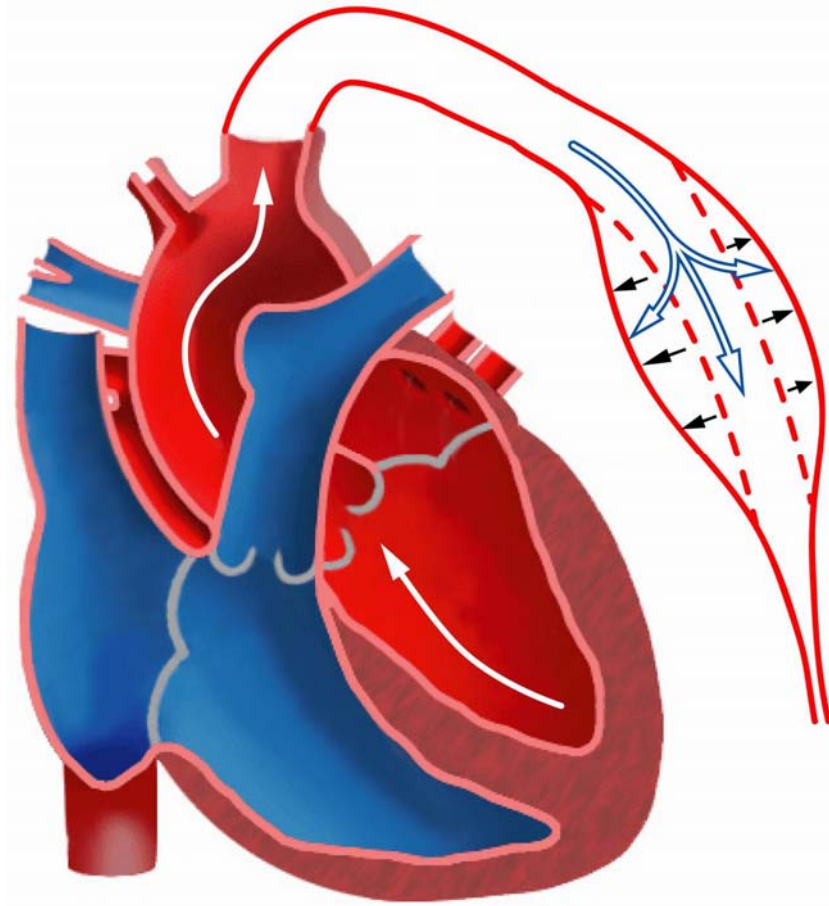
Figure 2-2 (a): When the ventricle contracts, the semilunar valve opens. Blood ejects into the aorta and arteries and makes them expanded. At the same time, the pressure stores in the elastic walls. This percussion produces the P wave.
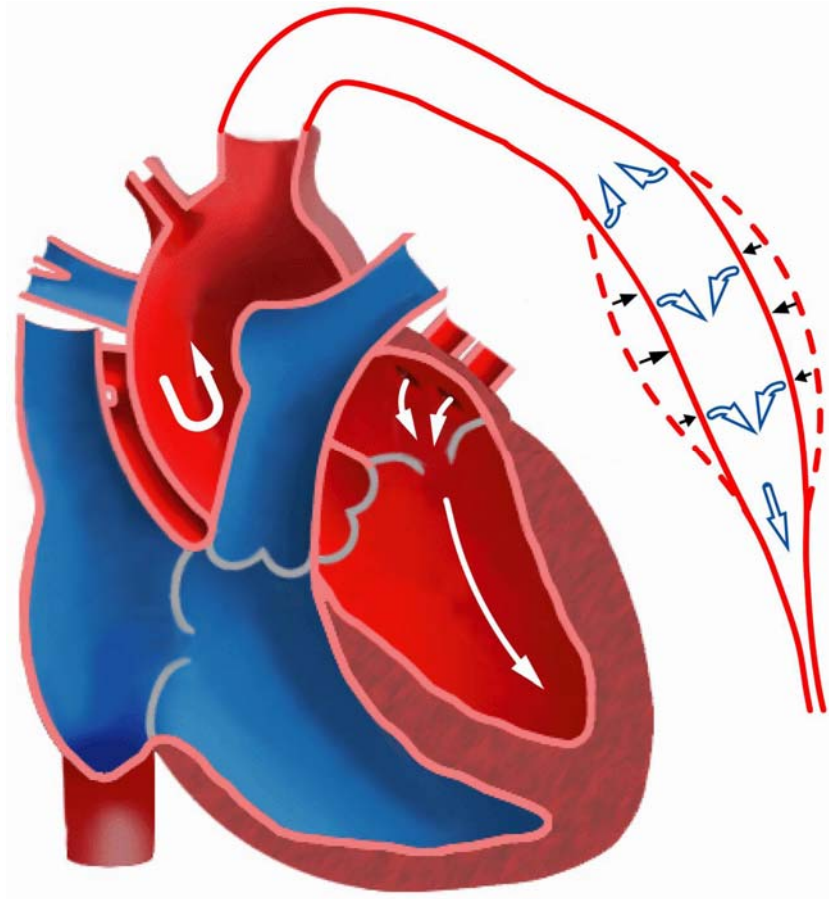
Figure 2-2 (b): Isovolumic ventricular relaxation makes the semilunar valve shut.

Elastic recoil of arteries sends blood forward into the rest of circulatory system. This

rebound makes the T wave and the closing of valve makes the D wave.

The second peak, called the Tidal wave (T wave), appears when blood hits the artery wall and rebounds. As a result, T wave is manifest if the artery possesses excellent elasticity that reflects low peripheral resistance of the circulatory system. On the other hand, an artery with a stiff wall makes the T wave propagate fast according to the Moens-Korteweg equation of wave velocity (Nichols et al., 1990; Khir et al., 2002). Accordingly, the T wave will merge with the P wave, which results in a wider P wave. The second parameter, $\frac{h_3}{h_1}$, where $h_3$ represents the height of T wave, is utilized to measure the effect of T wave. We thus expect a large $\frac{h_3}{h_1}$ for an arterial system with better elasticity. The valley height $h_4$ reveals the level of peripheral resistance (Fey, 2003; Milor, 1989). As the peripheral resistance increases (decreases), parameter $h_4$ increases (decreases) as well. The normalized parameter, $\frac{h_4}{h_1}$, is employed to measure the drift of peripheral resistance. Finally, when the aortic valve is closed, the Dicrotic wave (D wave) is generated. $h_5$ is the magnitude of D wave and the normalized parameter, $\frac{h_5}{h_1}$, represents the effect of D wave on arterial system. $h_5$ will decrease due to a stiff aorta or aortic regurgitation.

Fig. 2-3 displays the instrument for recording BPW from the wrist with a piezoelectric sensor. The sensor was manufactured by Skylark Company, with 3dB cutoff frequency at 10 KHz. The output is linearly dependent of the input when BP is below 1000 mmHg. The subject sat with one forearm on the desk. The angle between

upper arm and desk is about $120^{\circ}$. Pressure of the piezoelectric sensor on the wrist was adjusted for sufficient sensitivity of the BPW activity. The range of amplitude depends on the measuring position. In this study, we measured the BPW at the 'chun' position (Fig. 2-4). A well experienced TCM (Traditional Chinese Medicine) expert assisted us in the experimental setup and recording. He searched the "chun" position by palpating the wrist of the subject. The piezoelectric sensor was then attached to the proper position carefully identified by the expert. The pressure was adjusted until the output amplitude reached maximum, from which the amplitude recorded was in the range of 15 to 27 mmHg (Fey, 2003).



Figure 2-3: The acquiring instrument of blood pressure waveform.
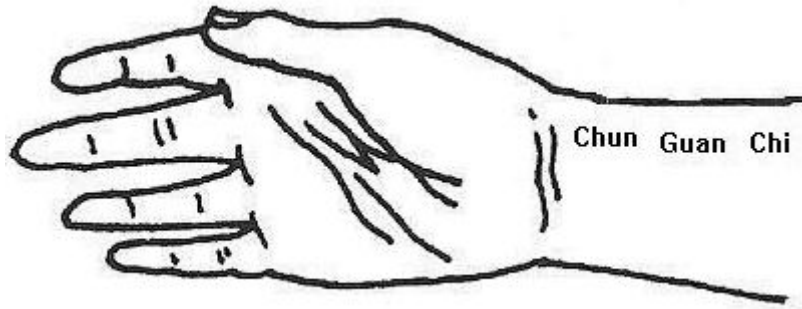
Figure 2-4: The measuring position on the wrist.

## 2.2.2 BPW parameters

The peak or valley positions in Figure 2-1 demonstrated by crosses are determined by the Matlab program for searching the local maximum or minimum. We first identify the P wave that is the most distinctive one. The starting point V1 of the whole period is about 0.1 sec prior to the P wave. The next step is to find the local minimum V3 at about 0.35 sec afterward from V1. Then the T wave between P wave and V3 is ready to be extracted. D wave comes after V3, that is identified by finding the null of waveform differentiation between V3 and the end of the BPW period. The time values of these specific points depend on the blood speed and the conditions of blood vessels. We referred to the paper by Xie (Xie et al., 2000) to check the standard time values of these parameters.

In this research, the above four parameters, $\dfrac{h_1}{t_1}$, $\dfrac{h_3}{h_1}$, $\dfrac{h_4}{h_1}$ and $\dfrac{h_5}{h_1}$ are used to

assess the status of cardiovascular system and corresponding parameters are defined as follows:

$$h_1 = \text{Peak height of P wave} - \text{Valley height of } V_1 \qquad (2.1)$$

$$h_3 = \text{Peak height of T wave} - \text{Valley height of } V_1 \qquad (2.2)$$

$$h_4 = \text{Valley height of } V_3 - \text{Valley height of } V_1 \qquad (2.3)$$

$$h_5 = \text{Peak height of D wave} - \text{Valley height of } V_3 \qquad (2.4)$$

$$t_1 = \text{Time of } V_1 - \text{Time of Peak of P wave} \qquad (2.5)$$

$$\text{Variation percentage} = \frac{\eta_{after-meditation} - \eta_{before-meditation}}{\eta_{before-meditation}} \times 100\%, \qquad (2.6)$$

where $\eta$ denotes one of the four parameters, $\frac{h_1}{t_1}, \frac{h_3}{h_1}, \frac{h_4}{h_1} or \frac{h_5}{h_1}$. Note that, due to the variations in recording system characteristics and physiological conditions of each subject, heights $h_3$-$h_5$ were normalized to within the range of 0 to 1. Normalization ensures an even comparison of BPW features in various recording sections. To avoid null denominator caused by the disappearance of *before-meditation* T wave (in the case, $h_3$=0), the variation percentage of $\frac{h_3}{h_1}$ is defined to be zero if T wave is absent before and after meditation. On the other hand, if T wave exists only after meditation, the variation percentage of $\frac{h_3}{h_1}$ will be assigned to 100% to avoid infinity.

## 2.3 Experiment and results

### 2.3.1  BPW signal processing

The blood pressure waveforms of radial artery non-invasively detected at wrist by piezo-electric transducer were recorded for 10 seconds and digitized at a sampling rate of 100 Hz. To reduce high frequency noise, a low-pass filter is designed with a 3dB cutoff frequency of 50 Hz. Because null baseline was required in the analysis, we removed the mean value of each BPW period in pre-processing. Accordingly, negative waveforms might appear. Note that non-constant, linear baseline drift sometimes interfered in the BPW (Fig. 2-5). The sources of interference include the body movement, heavy respiration, etc. The resulting artifacts might be false amplitude or position shift of peaks/valleys. Although removal of the baseline drift may help, we found it necessary to further correct the interference patterns. In that case, baseline removal involved a linear-regression method for baseline-drift detection.
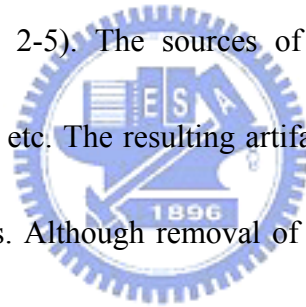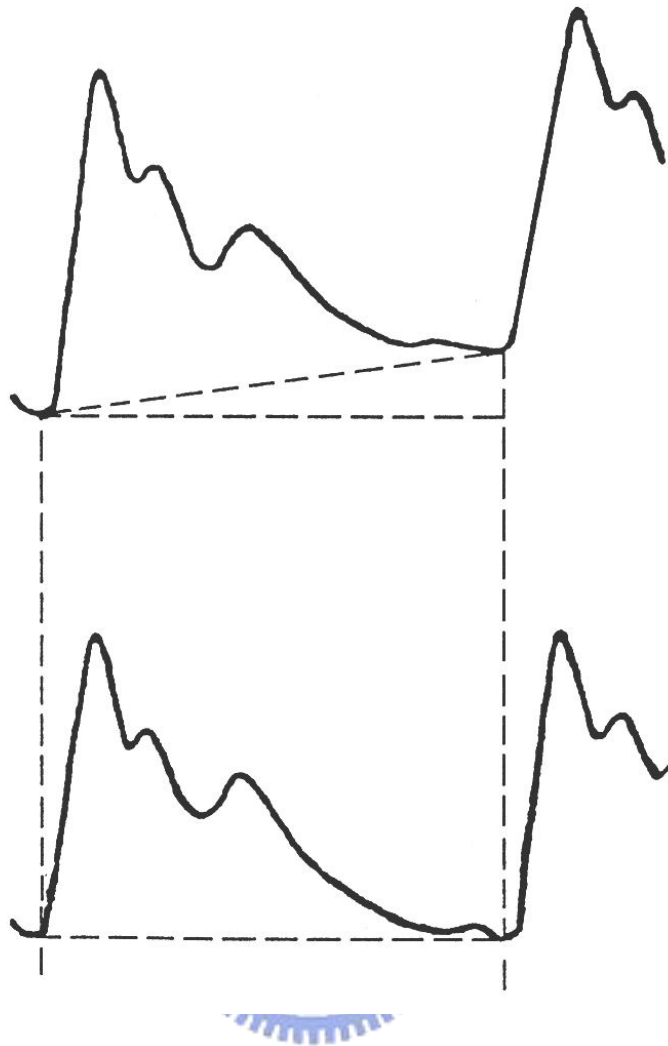
Figure 2-5: The linear baseline drift in the BPW (upper) and the result after removing it (lower).

The BPW recording instrument can only continuously trace for up to 10 seconds. BPW is a quasi-periodic signal with 10 to 16 complete cycles in a 10-second term. Here we averaged out the 10-16 cycles to get the final BPW for further quantification of embedded features. We thus can obtain triple to quadruple SNR (signal-to-noise ratio) that is linearly dependent of the square root of the number of measurements. The SNR level could fulfill our research requirements.

## 2.3.2 Subjects and recording paradigms

The participants were divided into two groups - 20 meditators and 20 normal, healthy people without any experience in meditation. In the experimental group, 13 females and 7 males with a mean age of 26.6±2.2 years participated. Their experiences in Zen-Buddhist practice span 6.9±3.3 years. The control group comprised 9 females and 11 males with a mean age of 25.2±1.8 years. All the meditation practitioners learned Zen-Buddhist meditation in the Taiwan Zen-Buddhist Association. Only experienced practitioners with more than 3 years of meditation experience were invited. The controls were graduate students of National Chiao-Tung University. No subjects had any cardiovascular disease in their medical histories.

Participants sat in an isolated space during the experiments. Blood pressure waves were recorded before and after the 40-minute main session (meditation or relaxation). In the main session, experimental group practiced Zen meditation, while controls sat in normal relaxed position with eyes closed.

## 2.4 BPW before and after meditation

Fig. 2-6 illustrates an example of the blood pressure waveform of meditator. The solid curve shows the *before-meditation* BPW, and the dashed one shows that after meditation. In Fig. 2-6, *after-meditation* P wave rises more steeply than the *before-meditation* one. For this particular subject, poor arterial elasticity makes the *before-meditation* T wave occur earlier and merge with P wave, resulting in a broadened P wave. In *after-meditation* BPW, the T wave becomes evident and distinguishable from the P wave, inferring that enhanced arterial elasticity is a consequence of meditation practice. Moreover, the $V_3$ valley descends (i.e., $h_4$ decreases) after meditation, indicating a decrease in peripheral resistance. The D wave magnitude is also strengthened after meditation. A typical example of 10-second BPW is shown in Fig. 2-7. Note that the pulse rate is slower after meditation, resulting in a phase difference between the two waves. In sum, the *after-meditation* BPW reflects a more robust cardiovascular system that could have been tuned up by the Zen meditation.
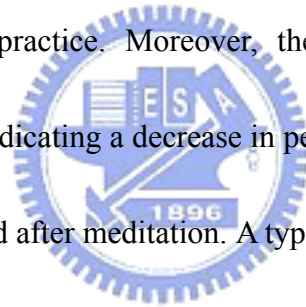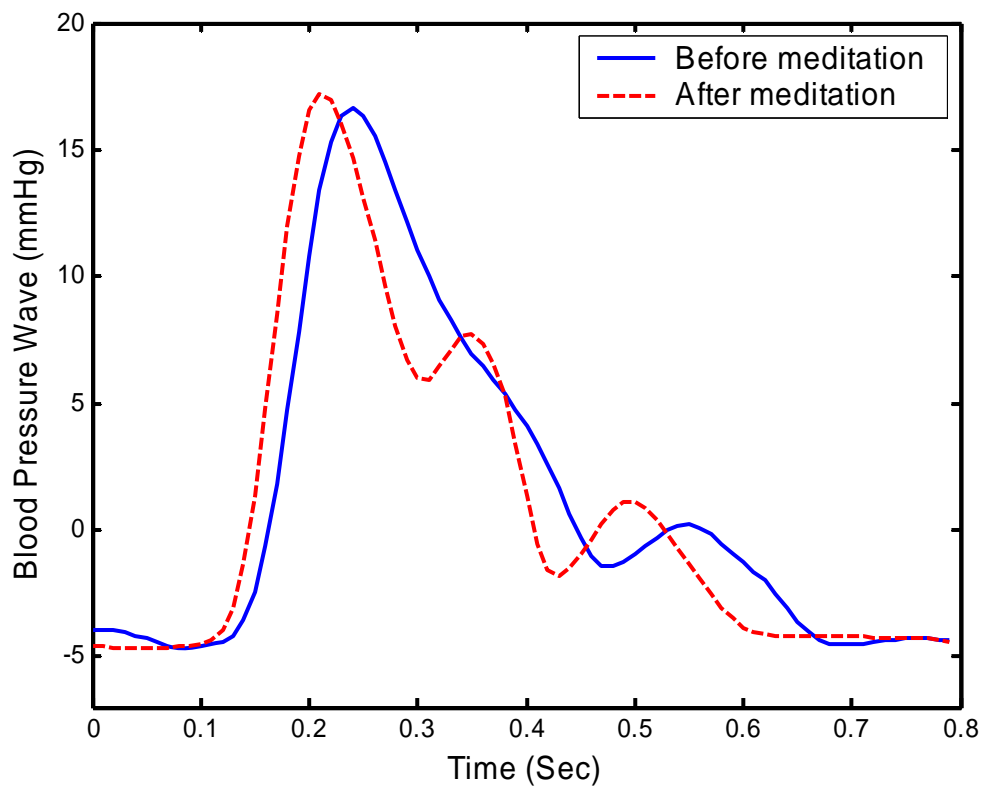
Figure 2-6: The *before-meditation* (solid curve) and *after-meditation* (dashed curve)

BPW for an experimental subject.
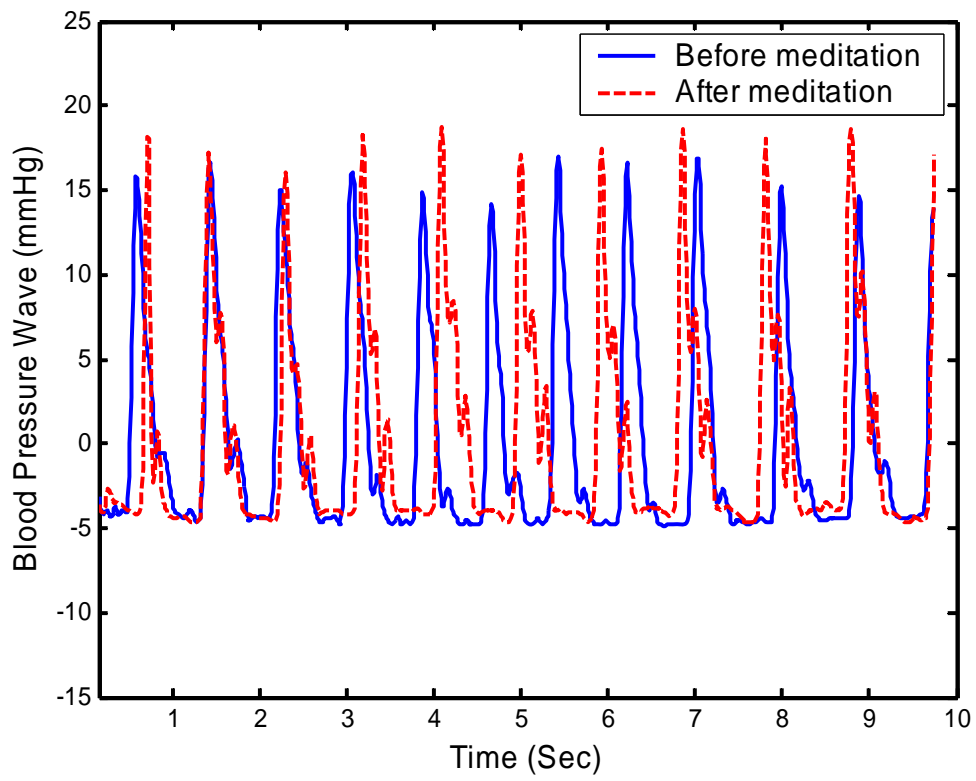
Figure 2-7: The ten-second typical BPW of one meditation practitioner.
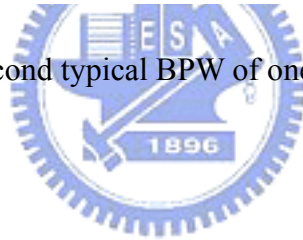
## 2.5 Inter-group comparison

Table 2-1 shows the results of the four parameters measured in both groups. The variation percentage of each parameter in each group is calculated by the formula (2.6). The *P*-values in Table 1 are evaluated using t-test, which is used to check whether the variation percentages show statistical differences between the groups. In this preliminary investigation, we concentrated on intra-subject differences between various experimental sections because the inter-subject variations in BPW were too complicated to manipulate.

In comparison with the control group, Zen-meditation practitioners have higher ranges of variation percentages in all four parameters. The performance details of each parameter are as follows: When considering the rising slope of P wave, $\frac{h_1}{t_1}$, that reflects the ejection ability of left ventricle or aorta elasticity, the experimental group had a mean increase from 390.8 to 435.1, a variation percentage of 11.7%, that was 5% higher than the variation percentage of control group. The second parameter $\frac{h_3}{h_1}$, measuring the effect of T wave, demonstrated distinct enhancement of arterial elasticity in the experimental group (three times the increasing rate of the control group). We discovered that even though some experimental subjects had vague T wave before meditation, it was often boosted after meditation. On the other hand, T wave variation of was not as obvious in the control group. We observed that some

26

control subjects did not even have a T wave before and after relaxation. If T waves merged with P waves, the parameter $\dfrac{h_3}{h_1}$ was considered to be zero. Next, the high decreasing rate of $\dfrac{h_4}{h_1}$ revealed reduced peripheral resistance after meditation. Finally, the increasing $\dfrac{h_5}{h_1}$ infers that Zen meditation significantly improves the quality of semilunar valves and arterial elasticity. The t-test results showed that all $P$-values were smaller than 0.05, further corroborating the significance of the improvement in the meditation group. In comparison with normal relaxation, Zen meditation may effectively improve the characteristics of cardiovascular system according to parameters extracted from blood pressure waves.

**Table 2-1. The statistical results of four parameters ($\frac{h_1}{t_1}$, $\frac{h_3}{h_1}$, $\frac{h_4}{h_1}$, $\frac{h_5}{h_1}$) and their variation percentages. P values are evaluated to show the statistical significance of discrimination between two groups.**

| | | $\frac{h_1}{t_1}$ | $\frac{h_3}{h_1}$ | $\frac{h_4}{h_1}$ | $\frac{h_5}{h_1}$ |
|---|---|---|---|---|---|
| Control group | Before Relaxation (Mean±Std.) | $380.6 \pm 26.0$ | $0.21 \pm 0.19$ | $0.27 \pm 0.08$ | $0.13 \pm 0.04$ |
| | After Relaxation (Mean±Std.) | $405.7 \pm 25.3$ | $0.25 \pm 0.19$ | $0.24 \pm 0.07$ | $0.15 \pm 0.07$ |
| | Variation percentage | 6.7% | 13.0% | $-9.3\%$ | 14.2% |
| Experimental group | Before Meditation (Mean±Std.) | $390.8 \pm 28.0$ | $0.20 \pm 0.19$ | $0.25 \pm 0.09$ | $0.13 \pm 0.04$ |
| | After Meditation (Mean±Std.) | $435.1 \pm 18.9$ | $0.36 \pm 0.13$ | $0.22 \pm 0.08$ | $0.16 \pm 0.03$ |
| | Variation percentage | 11.7% | 41.2% | $-13.5\%$ | 27.9% |
| P-value | | 0.005 ($< 0.05$) | 0.026 ($< 0.05$) | 0.032 ($< 0.05$) | 0.029 ($< 0.05$) |

# Chapter 3
# F-VEPs in Zen meditation

Observation of the inner-light perception in deep Zen meditation (Lo et al., 2003)

has aroused our attention. Based on the recording of F-VEPs (flash visual evoked

potentials), this study was thus designed to investigate the characteristics of visual

nervous pathway for the Zen-meditation practitioners (experimental group), in

comparison with that for the normal, healthy subjects (control group). Flash stimuli

were applied before, during and after meditation / relaxation in experimental / control

subjects. We focused on the F-VEPs at the occipital site Oz, central site Cz and frontal

site Fz.
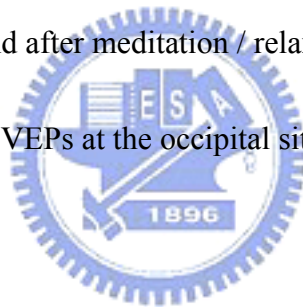
## 3.1 Background and motivation

During the past decades, a number of papers have reported the benefits of

meditation to the physiological and mental health, with particular emphasis on

transcendental meditation, Yoga meditation, and Japanese-Zen meditation. It is the

first attempt to investigate the electrophysiological signals of the orthodox

Zen-Buddhist practitioners. The main doctrine of Zen-Buddhist practice is to

transcend the physiological, mental, and subconscious states via Zen meditation that

enables the practitioners to reach a fully egoless, transcendental state (the Alaya state) (Lo et al., 2003).

Researchers have been probing into the physiological and psychological parameters during meditation for several decades (Jevning et. al., 1992; West, 1980). Some important results include: Wallace (Wallace, 1970) claimed the emergence of theta waves in the frontal area in transcendental meditation, Banquet observed the slowdown of alpha frequency and the increase of alpha amplitude as well as the occurrence of the rhythmic theta trains (Banquet, 1973). Recently, Lutz and et al. found that long-term Buddhist practitioners self-induced sustained high-amplitude, gamma-band EEG and phase-synchrony during meditation (Lutz and et al., 2004). These patterns obviously occurred at the lateral fronto-parietal electrodes. Travis found several physiological markers including the decrease of respiration rate, higher respiratory sinus arrhythmia amplitudes, higher alpha coherence, etc (Travis, 2001).

In addition, ERPs (evoked response potential) used to explore the underlying neuron activities in meditation were investigated. Zhang claimed the increase of F-VEP amplitudes of Qigong practitioners under meditation (Zhang, 1993). In Xu et, al.'s research, increase of amplitude and decrease of latency were reported (Xu et al., 1998). Furthermore, auditory evoked potential (AEP) under meditation has also been studied to investigate the meditation effects on the brainstem auditory response

(McEvoy et al., 1980; Tells et al., 1994).

The paper survey given above shows a particular phenomenon of meditation, that is, its effects on the frontal cortex. The transcendental state of Zen meditation, in fact, reflects that the human life system turns off its physical and mental sensors, leaves off the message transmission from outside world, and keeps subconscious tranquil. When further attaining the deeper meditation state, practitioners often ignite their *inner energy*, accompanied with the experience of perceiving the *inner light* (Lo et al., 2003). Base on the observation of frontal EEG and the common experiences of *inner-light* perception, we hypothesized that meditation would affect the visual neuron pathway, and the effect might be modulated by the meditation effects in the frontal area of the cortex.
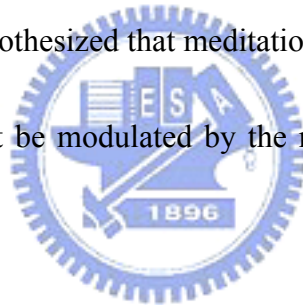
Accordingly, this study aimed to investigate the meditation effects on visual neuron pathway by quantitatively analyzing the visual evoked potentials (VEPs). Owing to the limitation that meditators must close their eyes during meditation, we employed the flashed light as the visual stimulus and recorded the flash visual evoked potential (F-VEP), with particular emphasis on channels Oz, Cz, and Fz.

## 3.2 Experimental setup and procedure

This study involves 30 experimental subjects (meditators) and 30 control

subjects (normal, healthy people without any experience in meditation). In the experimental group, 15 females and 15 males at the mean age of 28.7±4.6 years participated. Their experiences in Zen-Buddhist practice span 6.6±4.1 years. The control group consists of 9 females and 21 males at the mean age of 24.1±1.6 years. EEG and F-VEP were recorded within the frequency range from 0.15Hz to 50Hz. The sampling rate is 1000Hz. We applied the 30-channel recording montage with the ground at the forehead and the reference as the linked mastoids.

F-VEPs were recorded before, during and after the main session (meditation or relaxation), that is called the pre-, mid-, or post-session. Continuous, 100 flash stimuli were applied to the subject in each session. The flash light was 10 µs in duration and 1 Hz in frequency produced by a xenon lamp that was placed 60 cm in front of the subjects' eyes. These parameters were referred to the standard procedures (Adrian and Mathews, 1934; Cigánek, 1961; Odom et al., 2004). We averaged these 100 trials to get the averaging F-VEP in each session. Subjects sat in a isolated space during the recording. Each recording lasted for about one hour. The course included 10min pre-session, 40min mid-session, and 10min post-session recording. In the mid-session period, experimental subjects practiced the Zen meditation, while control subjects sat in normal relaxed position with eyes closed. During the meditation, the subject sat, with eyes closed, in the full-lotus or half-lotus position. In the begining of meditation,

the subjects focused on the Navel Chakra and regulated their respiration. Navel Chakra is regarded as an important *switch* that activates the other Chakras. After igniting the Navel Chakra, meditators focused on the Zen Chakra or Dharma Chakra to empty the thought.

## 3.3 Results and inter-group comparison

Figures 3-1 and 3-2 are the averaged F-VEPs on Oz, Cz and Fz of one experimental and one control subject, respectively. The dotted, solid and dashed lines represent respectively the pre-, mid-, and post-session F-VEPs. Tables 3-1 and 3-2 list the average ratios of mid- to pre- and post- to mid-session latencies and amplitudes for both group. The p values are calculated by *paired t-test* and *t-test*.

The peak numbers are named according to the visual evoked potential standard (Odom et al., 2004). From Table 3-1, we can examine the variations in latencies between sessions or between groups.
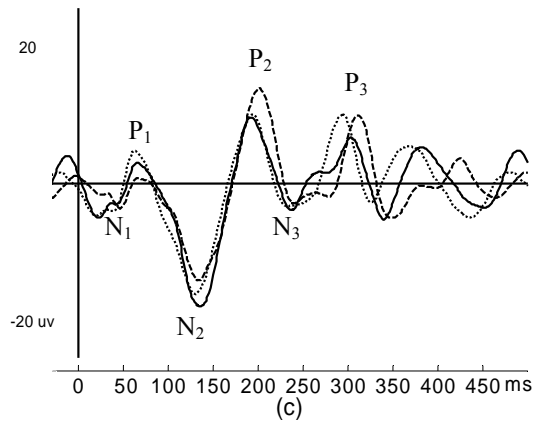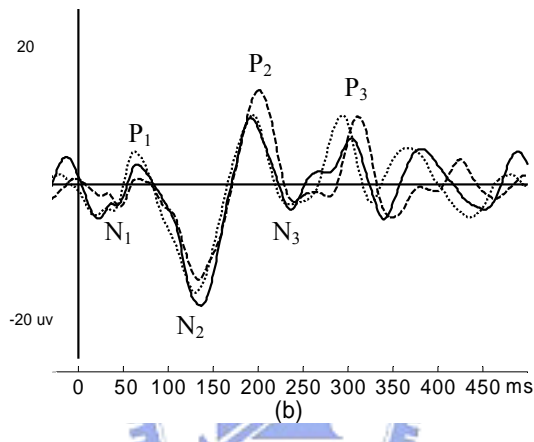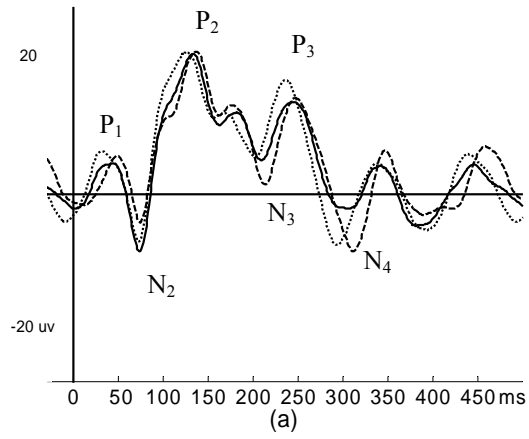
Figure 3-1: The F-VEP on (a)Oz (b)Cz (c)Fz of a meditator.
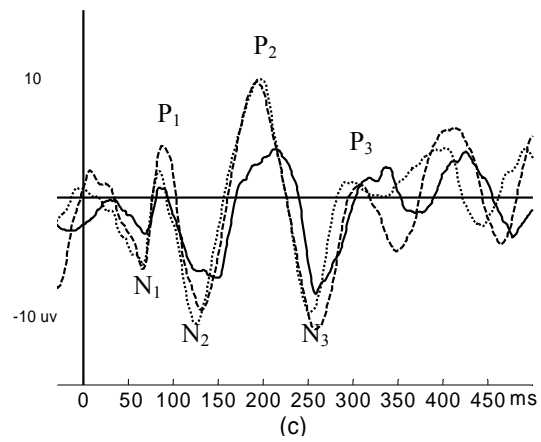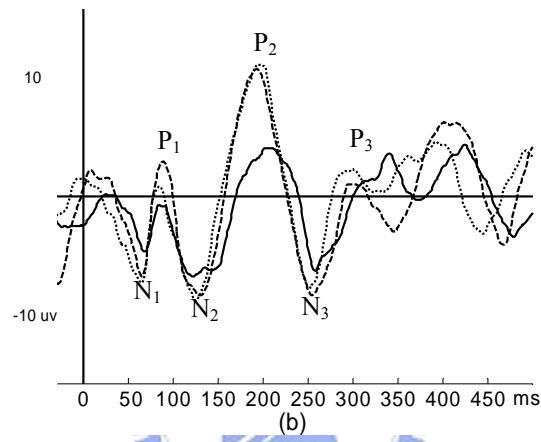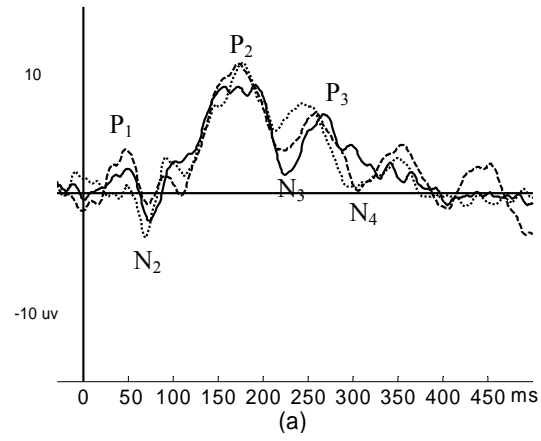
Figure 3-2: The F-VEPs on (a)Oz (b)Cz (c)Fz of a control subject.

Table 3-1. Average ratios of peak latencies (NS: not significant).

| Item | | Exp group | | | Ctrl group | | | t-test | |
|---|---|---|---|---|---|---|---|---|---|
| | | mid/pre (%) | post/mid (%) | P value (paired t-test) | mid/pre (%) | post/mid (%) | P value (paired t-test) | mid/pre | post/mid |
| Oz | P1 | 106.45 | 98.79 | NS | 110.79 | 96.36 | NS | NS | NS |
| | N2 | 100.65 | 100.16 | NS | 103.40 | 99.94 | NS | NS | NS |
| | P2 | 103.52 | 99.13 | **0.001\*** | 104.60 | 100.72 | NS | NS | NS |
| | N3 | 101.91 | 99.99 | NS | 100.00 | 101.59 | NS | NS | NS |
| | P3 | 101.34 | 99.85 | NS | 100.24 | 101.47 | NS | NS | NS |
| | N4 | 100.57 | 99.81 | NS | 100.62 | 99.51 | NS | NS | NS |
| Cz | N1 | 103.47 | 101.77 | NS | 129.77 | 98.57 | **0.009\*** | **0.008\*** | NS |
| | P1 | 100.72 | 102.66 | NS | 109.84 | 106.50 | NS | **0.009\*** | NS |
| | N2 | 101.15 | 99.61 | NS | 102.68 | 98.82 | NS | NS | NS |
| | P2 | 101.03 | 99.93 | NS | 102.51 | 100.00 | NS | NS | NS |
| | N3 | 103.41 | 100.09 | NS | 105.02 | 100.40 | NS | NS | NS |
| Fz | N1 | 105.77 | 104.65 | NS | 111.05 | 92.74 | **0.040\*** | NS | **0.042\*** |
| | P1 | 102.32 | 100.75 | NS | 109.13 | 97.42 | **0.024\*** | **0.024\*** | NS |
| | N2 | 100.98 | 100.38 | NS | 102.19 | 99.59 | NS | NS | NS |
| | P2 | 100.50 | 99.30 | NS | 103.65 | 99.47 | NS | NS | NS |
| | N3 | 99.81 | 100.29 | NS | 105.68 | 98.30 | **0.021\*** | **0.042\*** | NS |

We summarize some important findings as follows (exp: experimental group, cnt: control group).

(1) Significant variations in latency are: (exp) P2 at Oz; (cnt) N1 at Cz, P1 and N3 at Fz. Note that all the latencies of these components increase during meditation/relaxation and decrease in the post-session.

(2) Two groups show different trends in the latency ratios: (mid/pre) N1 and P1 at Cz; P1 and N3 at Fz. The latencies of these components in the control group show considerable increasing, whereas the changes of experimental group are not apparent. (post/mid) N1 at Fz: the latency of the experimental group increased, but it decreased in the control group.
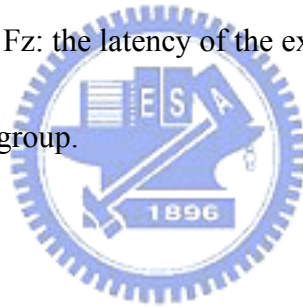
Table 3-2. Average ratios of peak amplitudes (NS: not significant).

| Item | | Exp group | | | Ctrl group | | | t-test | |
|------|------|------|------|------|------|------|------|------|------|
| | | mid/pre (%) | post/mid (%) | P value (paired t-test) | mid/pre (%) | post/mid (%) | P value (paired t-test) | mid/pre | post/mid |
| Oz | P1-N2 | 112.89 | 102.20 | NS | 121.64 | 100.98 | NS | NS | NS |
| | N2-P2 | 104.98 | 104.86 | NS | 110.82 | 115.67 | NS | NS | NS |
| | P2-N3 | 109.57 | 100.72 | NS | 121.50 | 116.99 | NS | NS | NS |
| | N3-P3 | 82.93 | 128.93 | **0.016*** | 124.61 | 111.83 | NS | **0.006*** | NS |
| | P3-N4 | 89.10 | 126.96 | **0.037*** | 132.79 | 116.69 | NS | **0.002*** | NS |
| Cz | N1-P1 | 95.91 | 114.92 | NS | 108.88 | 103.98 | NS | NS | NS |
| | P1-N2 | 112.49 | 90.94 | NS | 84.88 | 117.91 | **0.038*** | **0.019*** | **0.031*** |
| | N2-P2 | 102.87 | 107.42 | NS | 98.14 | 115.47 | NS | NS | NS |
| | P2-N3 | 125.30 | 119.52 | NS | 113.01 | 130.20 | NS | NS | NS |
| Fz | N1-P1 | 112.13 | 113.35 | NS | 106.25 | 109.02 | NS | NS | NS |
| | P1-N2 | 100.18 | 101.09 | NS | 84.82 | 113.64 | **0.047*** | **0.045*** | NS |
| | N2-P2 | 99.62 | 110.85 | NS | 105.07 | 103.83 | NS | NS | NS |
| | P2-N3 | 105.58 | 122.10 | NS | 121.35 | 114.16 | NS | NS | NS |

From Table 3-2, we can examine the variations in amplitudes between sessions or between groups. We summarize some important findings as follows.

(1) Significant variations in amplitude are: (exp) N3-P3 and P3-N4 at Oz; (cnt) P1-N2 at Cz and Fz. The amplitudes of these components decrease during meditation/relaxation and increase afterwards.

(2) Two groups show different trends in the magnitude ratios: (mid/pre) N3-P3 and P3-N4 at Oz; P1-N2 at Cz and Fz; (post/mid) P1-N2 at Cz. In experimental group, the amplitudes of N3-P3 and P3-N4 at Oz are decreased under meditation, but the trends are opposite under relaxation in the control group. The amplitudes of P1-N2 on Cz and Fz are increased in experimental group but decreased in the control group during meditation/relaxation. Furthermore, after meditation/relaxation, P1-N2 at Cz is decreased in the experimental group and is increased in the control group.
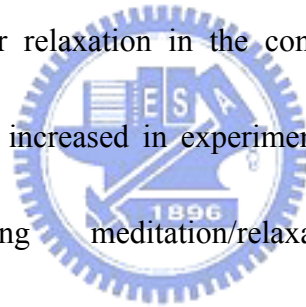
# Chapter 4

# Spatial Focalization of Zen-Meditation Brain Based on EEG

The aim of this study is to report our preliminary results of investigating the spatial focalization of Zen-meditation EEG (electroencephalograph) in alpha band (8-13 Hz). For comparison, the study involved two groups of subjects, practitioners (experimental group) and non-practitioners (control group).
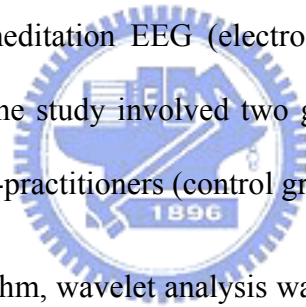
To extract EEG alpha rhythm, wavelet analysis was applied to multi-channel EEG signals. Normalized alpha-power vectors were then constructed from spatial distribution of alpha powers, that were classified by Fuzzy C-means based algorithm to explore various brain spatial characteristics during meditation (or, at rest). Optimal number of clusters was determined by correlation coefficients of the membership-value vectors of each cluster center.

## 4.1 Background and motivation

Numerous studies have reported the physiological and psychological effects of

40

meditation. Scientists have corroborated that meditation considerably lowered down the levels of respiration rate, heart rate, spontaneous skin conductance response and cortisol (Dillbeck and Orme-Johnson, 1987; Jones, 2001). Other researches reported that meditation was useful in treating some medical problems such as hypertension (Walton et al., 1995; Barnes et al., 2001), anxiety (Lindberg, 2005), pressure (Shetty, 2005), and even tumors (Ott et al., 2006). In psycho-neurology, EEG becomes an important tool to monitor the meditation effects on the neural systems.

According to those literatures, the most common phenomenon is the increase of alpha-band power and alpha coherence in the frontal areas (Aftanas and Golocheikine, 2001; Travis et al., 2002; Murata et al., 2004; Takahashi et al., 2005). Alpha activities are normally recorded on the posterior scalp regions for normal, healthy adults with eye-closed relaxation under conditions of physical relaxation and relative mental inactivity. In Cantero et al.'s research, they concluded that alpha rhythm could be the *baseline* of brain activity when sensory inputs are very few at the state of relaxed wakefulness (Cantero, Atienza, Salas and Gómez, 1999). Cantero et al. provided evidence for the alpha power modulation and different scalp distributions at a particular cerebral arousal state (Cantero, Atienza, Gomez and Salas, 1999). Correlation between cognition and alpha variation during meditation was studied by some researchers. Aftanas & Golocheikine claimed that turning off external attention

41

during meditation reflected the increasing power of slow alpha in the frontal areas (Aftanas et al., 2001). Since alpha variations are the common characteristic during meditation, investigation of alpha spatial-temporal traits is important for further understanding the neural-physiological effects of meditation.

Among various meditation techniques, we focus on Zen meditation that has been becoming popular in Taiwan. During meditation, meditators first transcend their physical and mental perceptions via particular mind-focusing technique, leave off the message transmission from outside world, and concentrate their attention on some particular Chakras (Lo et al., 2003).

Exploration of the meditation alpha activities has been focused on the change of alpha power and coherence, with few studies on the spatial-temporal behavior. Owing to the particular cognitive significance of alpha rhythms, investigating the distribution of alpha band might help understanding the meditation effects on the cortical activation. The aim of this study is thus to investigate the temporal evolution of spatial characteristics of alpha rhythms under Zen meditation.

In the following section, we introduce the methods for multi-channel meditation EEG processing and analysis, including wavelet transform for identifying alpha-dominated sections and Fuzzy C-means for classifying the feature vectors that represent the spatial distribution of alpha rhythms. Finally, we discuss the difference

of spatial characteristics between experimental group (Zen meditators) and control

group (non-meditators).

## 4.2 Proposed schemes

### 4.2.1 Wavelet Transform

Spectrum analysis based on Fourier Transform (FT) has been the most popular

method for identifying various EEG rhythms. However, FT can not resolve the

time-varying spectral properties of EEG. Wavelet Transform (WT) is one of the

approaches developed to solve the problem (Daubechies, 1992). WT decomposes a

signal into scaled, time-shifted version of the pre-designed wavelet prototype. WT

possesses the capability of local analysis as well as high flexibility in terms of

scalability in resolution. However, choosing an appropriate wavelet prototype is

always the issue firstly encountered. A rational thought is to choose a wavelet model

with its pattern matching the shape of the component to be analyzed. Accordingly, the

wave shape of Daubechies 6 (Db 6) low-pass filter was selected in this study.

Furthermore, Daubechies wavelets are used due to their properties, including good

regularity for high number of moments (Dragotti and Vetterli, 2003).

### 4.2.2 Alpha detection

A number of alpha detection algorithms have been developed in both time and

frequency domains. Due to the time-varying spectral behavior of alpha patterns, a wavelet-based algorithm becomes appealing for alpha detection.

To decompose the EEG, discrete wavelet transform (DWT) was implemented by the typical pyramidal structure (order 2), with a window size of 1 second and no overlap. We then calculated the wavelet coefficients corresponding to the delta ($\delta$: 3.5 Hz or less), theta ($\theta$: 4~7.5 Hz), alpha ($\alpha$: 8~13 Hz), beta ($\beta$: 14~30 Hz) and gamma ($\gamma$: above 30 Hz) band. Finally, EEG rhythm in each particular band was reconstructed. Define the alpha-power percentage $\rho$ below,

$$\rho = \frac{p_\alpha}{p_\delta + p_\theta + p_\alpha + p_\beta + p_\gamma} \times 100\% \qquad (4.1)$$

where $P_\alpha$ denotes the power of the reconstructed $\alpha$ wave, and so on.

Consider an EEG epoch. If the alpha-power percentage $\rho$ is greater than a pre-defined threshold $\theta_1$ ($\theta_1$=50% in this study), it is considered as an alpha-dominated epoch. Figure 1 displays alpha-power percentages varying with time.

From Figure 1, alpha apparently dominated the last 3 seconds ($\rho > 50\%$), that were to be extracted for further spatial analysis. All the 30-channels were examined to identify the alpha-dominated epochs. Those epochs with at least one channel satisfying $\rho > 50\%$ were extracted. Next the alpha-power vector is defined as

$$p_{\alpha i} = [\, p_{\alpha i1} \qquad p_{\alpha i2} \qquad p_{\alpha i3} \quad \cdots \quad p_{\alpha i30} \,] \qquad (4.2)$$

where $P_{\alpha i}$ is a vector containing the 30-channel alpha powers for the $i^{th}$ epoch, with its

element $P_{\alpha ij}$ representing the alpha power of the $j^{th}$ channel. Final feature vector was obtained by normalizing the alpha-power vector based on the pool of all vectors extracted.
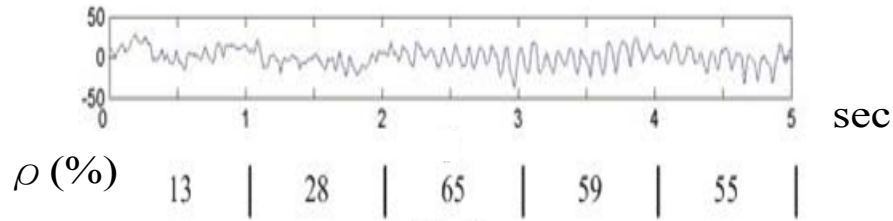


Figure 4-1: A section of 5-sec EEG. The numbers listed below are the alpha-power percentages.

## 4.2.3 Fuzzy C-means

Fuzzy c-means (FCM) is a data clustering method wherein each data point belongs to a cluster to some degree specified by a membership value (Bezdek, 1973). We utilized FCM to classify the input feature vectors (normalized alpha-power vectors). In FCM, number of clusters needs to be determined first. We proposed the idea of evaluating correlation coefficients to estimate the appropriate number of clusters. First, with an initial guess (>5), we can derive the membership value for each sample $x_j$:

$$\chi_{ij} = \left[ \sum_{l=1}^{c} \left[ \frac{d_{ij}}{d_{lj}} \right]^{\frac{2}{\beta-1}} \right]^{-1} \tag{4.3}$$

where $\chi_{ij}$ is the membership value of sample $x_j$ with the center $y_i$, $d_{ij}$ is the distance between $x_j$ and $y_i$, $c$ is the number of clusters, and $\beta$ is the fuzziness coefficient. Each

45

center $y_i$ has its membership-value vector,

$$\chi_i = \begin{bmatrix} \chi_{i1} & \chi_{i2} \cdots \chi_{im} \end{bmatrix} \tag{4.4}$$

Here $m$ is the number of extracting vectors. The correlation coefficient is

$$R(\chi_i, \chi_j) = \frac{C(\chi_i, \chi_j)}{\sqrt{C(\chi_i, \chi_i)C(\chi_j, \chi_j)}} \tag{4.5}$$

where $C(\chi_i, \chi_j) = E\big[(\chi_i - \mu_i)(\chi_j - \mu_j)\big]$ is the covariance matrix.

If $R(\chi_i, \chi_j)$ is larger than the threshold $\theta_2$ (in statistical reason, we set $\theta_2 = 0.3$ for the side line between strong and weak correlation), $y_i$ and $y_j$ are too close, and the number of cluster $c$ must be reduced by 1.

First we checked the performance of our algorithm by analyzing 800 real EEG epochs. Normalized alpha-power vector is illustrated by colored brain mapping. Figure 4-2 displays the results of classifying the alpha-power mappings into 4 clusters. Figure 4-2 and 4-3 display some sample brain mappings in each cluster for 4 and 3 clusters, respectively. Table 4-1 lists the correlation coefficients between clusters $i$ and $j$, $1 \le i, j \le 4$ (assume 4 clusters).

Cluster #1

Cluster #2
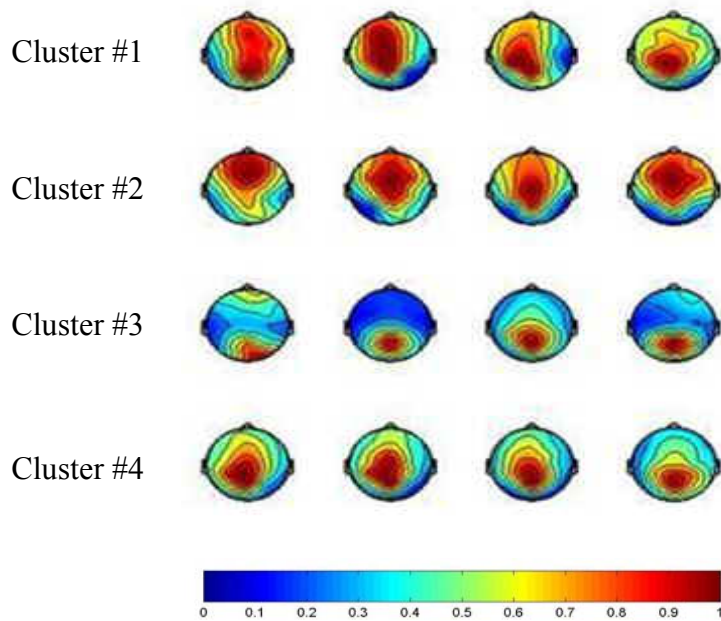
Cluster #3

Cluster #4

Figure 4-2: The results of 4 clusters

Table 4-1: The correlation coefficients (4 clusters)

| Cluster | 1 | 2 | 3 | 4 |
|---------|-------|-------|-------|-------|
| 1 | | 0.67 | -0.86 | -0.32 |
| 2 | 0.67 | | -0.73 | -0.64 |
| 3 | -0.86 | -0.73 | | 0.04 |
| 4 | -0.32 | -0.64 | 0.04 | |

Apparently, mappings in cluster #1 are very similar to those in cluster #2, and a large correlation coefficient $R(\chi_1, \chi_2) = 0.67$ is obtained. Accordingly, number of clusters should be reduced. Figure 4-3 shows the results of 3 clusters. Table 4-2 shows the correlation coefficients for the 3-cluster case. Note that none of these coefficients exceeds $\theta_2$, that indicates the number of clusters $c = 3$ is appropriate for the sample pool analyzed. The example above demonstrates the strategy of determining the appropriate number of clusters. Flowchart of the algorithm is shown in Figure 4-4.



Figure 4-3: The results of 3 clusters
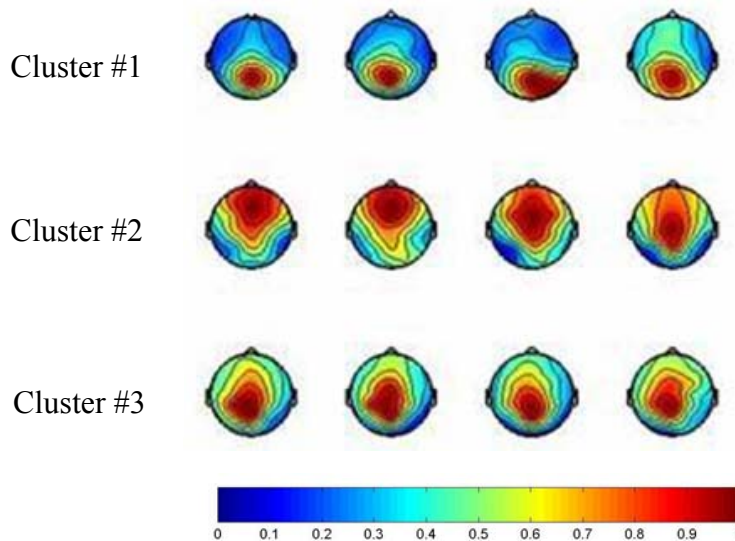
Table 4-2: The correlation coefficients (3 clusters)

| Cluster | 1 | 2 | 3 |
|---------|-------|-------|-------|
| 1 | | -0.80 | -0.51 |
| 2 | -0.80 | | -0.11 |
| 3 | -0.51 | -0.11 | |
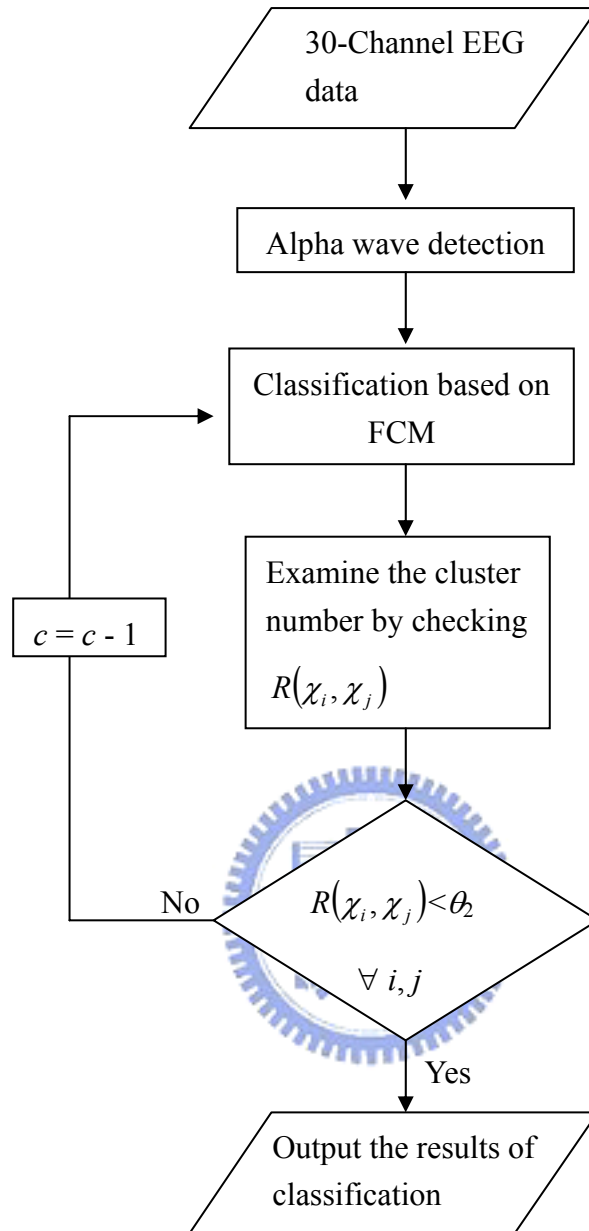
Figure 4-4: Flowchart of the proposed algorithm

## 4.3 Subjects and recording setup

This study involved 10 experimental subjects (Zen meditators) and 10 control subjects (normal, healthy people without any experience in meditation). Experimental group included 3 females and 7 males at the average age of 28.9±3.2 years. Their experiences in Zen-Buddhist practice span 7.6±4.5 years. Control group consisted of 4 females and 6 males at the average age of 25.9±5.2 year.

EEG was recorded within the frequency range from 0.15Hz to 50Hz, with a sampling rate of 512 Hz. We applied the 30-channel recording montage, based on the 10-20 system, with the ground at the forehead and the linked mastoids as the reference.
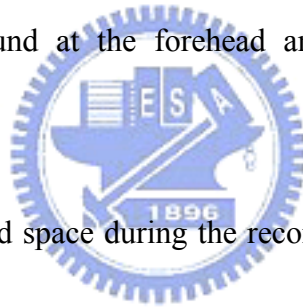
Subjects sat in an isolated space during the recording. Each recording lasted for about 34 minutes, including 2-minute pre-session, 30-minute main-session, and 2-minute post-session recording.

In the main-session period, experimental subjects practiced the Zen meditation, while control subjects sat in normal, relaxed position with eyes closed. During the meditation, experimental subject sat in the full-lotus or half-lotus position, with eyes closed. While before and after the main-session period, both experimental and control subjects closed their eyes and relaxed.

## 4.4 Results

Figs. 4-5 to 4-7 plot the results for one experimental subject (cluster number c=3). Totally 709 alpha-power vectors were detected and analyzed. Only a portion of alpha-power brain mappings are displayed for each cluster.

Table 4-3 lists the Euclidean distances between different cluster centers. Standard deviation of the distances of all vectors away from the cluster center is computed for each cluster (Table 4-4). According to Tables 4-3 and 4-4, distances between cluster centers are greater than three times of the standard deviations. Evidently, FCM successfully separated these clusters.
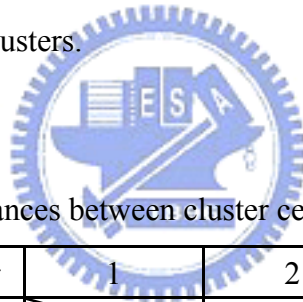
Table 4-3: The Euclidean distances between cluster centers

| Cluster \ Cluster | 1 | 2 | 3 |
|---|---|---|---|
| 1 | | 1.474 | 0.765 |
| 2 | 1.474 | | 0.895 |
| 3 | 0.765 | 0.895 | |

Table 4-4: The standard deviation of the distances of each sample to its center

| Cluster | Number of samples | Standard deviation of the distances |
|---|---|---|
| 1 | 266 | 0.250 |
| 2 | 246 | 0.232 |
| 3 | 197 | 0.242 |

To investigate the spatiotemporal evolution of alpha activities, we employed the color-chart illustration with red, blue and green indicating the emergence of brain mappings belonging to cluster #1, #2 and #3, respectively (Figure 4-8). Black indicates the non-alpha epochs.

From this chart, we could assess the alpha distribution easily. For instance, we could find frontal alpha (class #1) emerged more often in the middle and non-alpha presented in the late phase of the main-session. The statistical analysis of spatiotemporal distribution of alpha activities for both groups will be discussed in the next section.
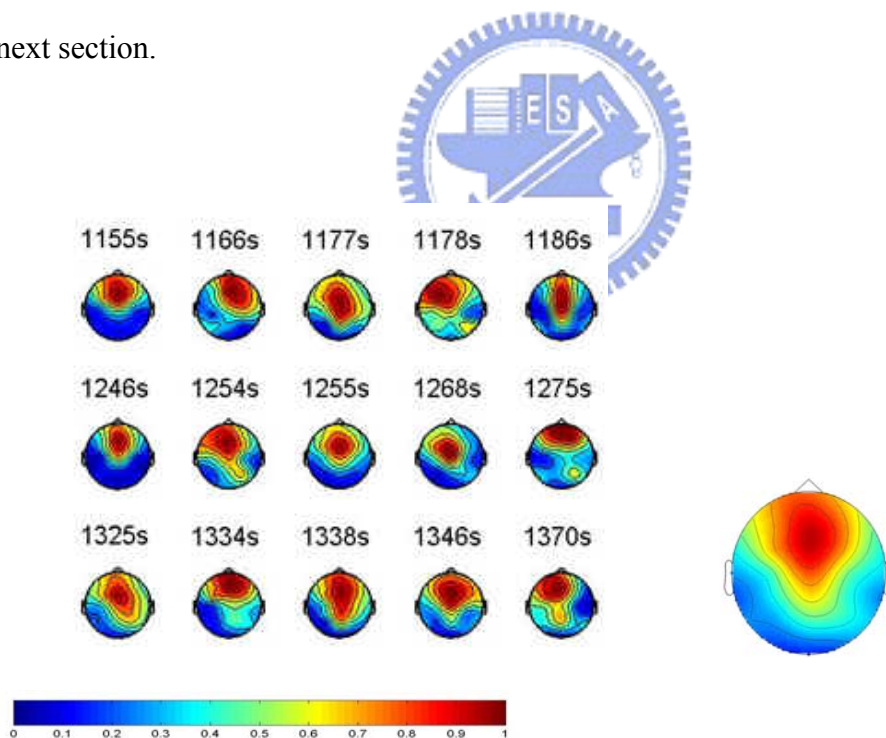


Figure 4-5: Selected samples (three rows) and the center of Cluster #1. The numbers above the samples are the time indices (in sec).
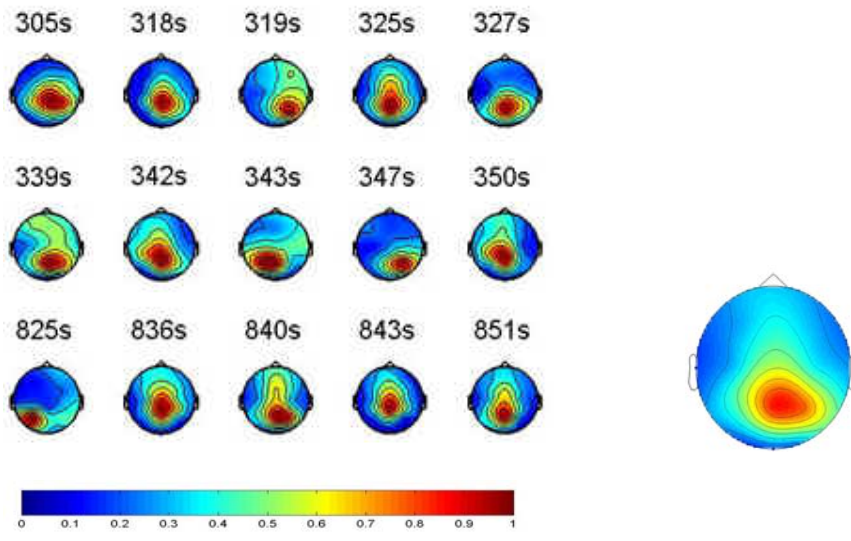
Figure 4-6: Selected samples (three rows) and the center of Cluster #2. The numbers above the samples are the time indices (in sec).
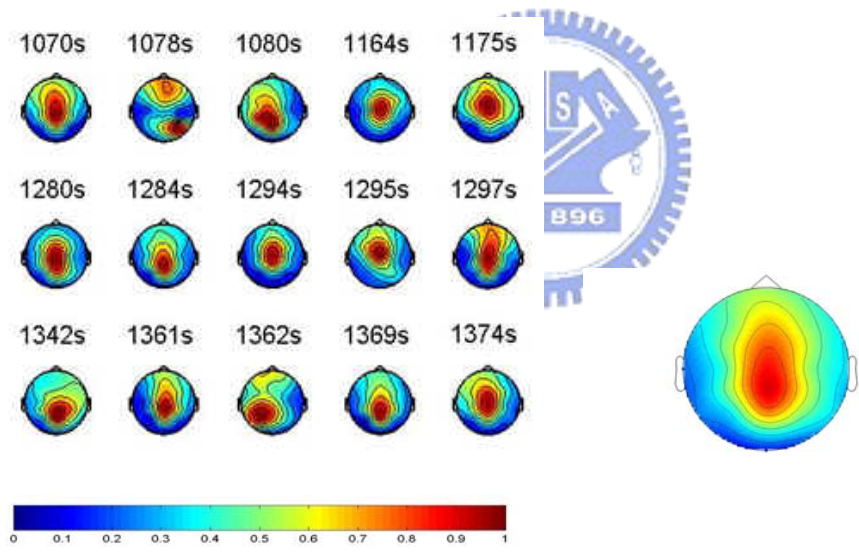


Figure 4-7: Selected samples (three rows) and the center of Cluster #3. The numbers above the samples are the time indices (in sec).
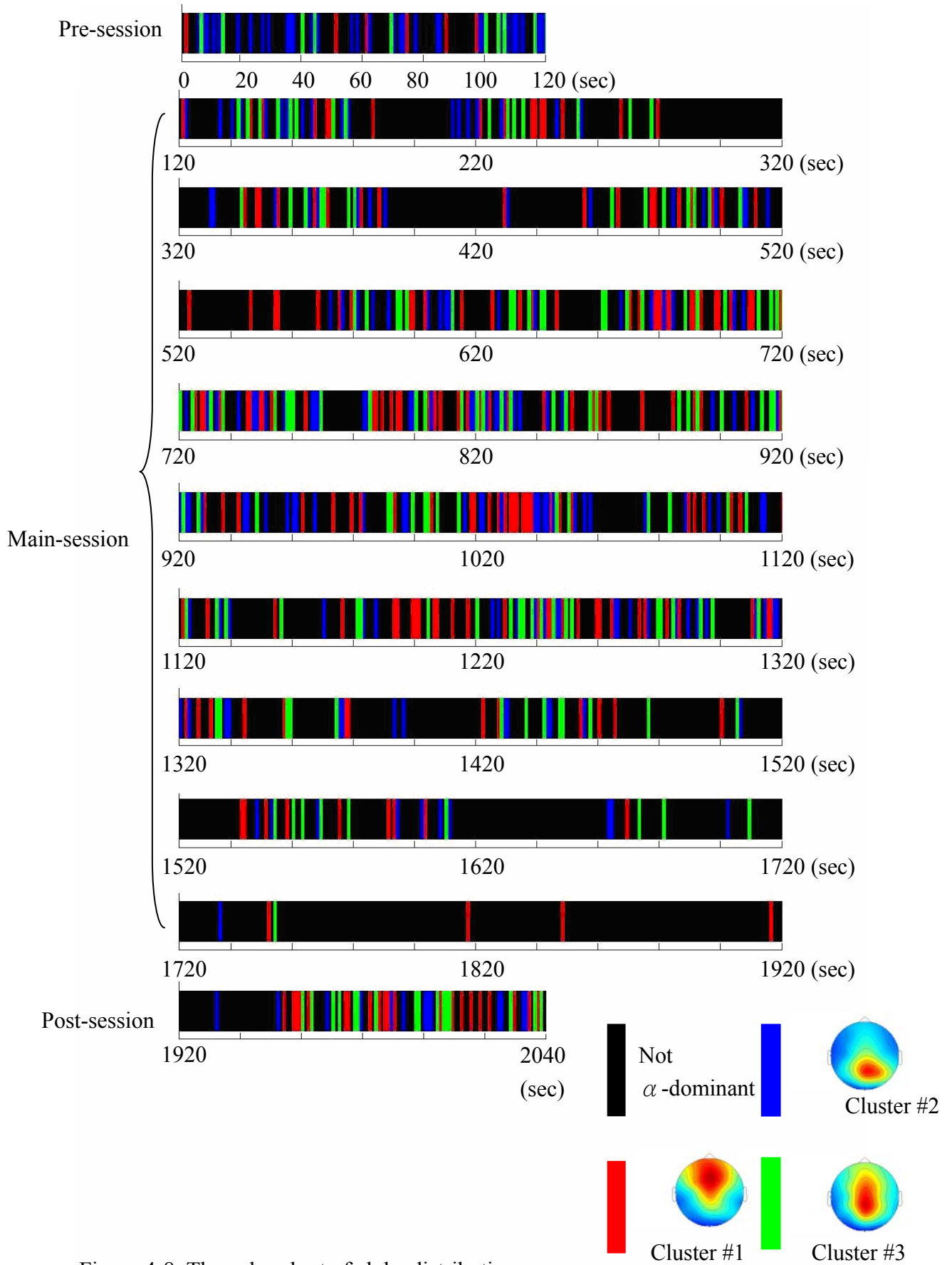
Figure 4-8: The color chart of alpha distribution

To investigate the focalization of alpha activity, we divided the scalp into six areas (Figure 4-9) representing six categories. The classification was based on 'peak' location since it reflected the source focalization (Lehmann, 1990a).
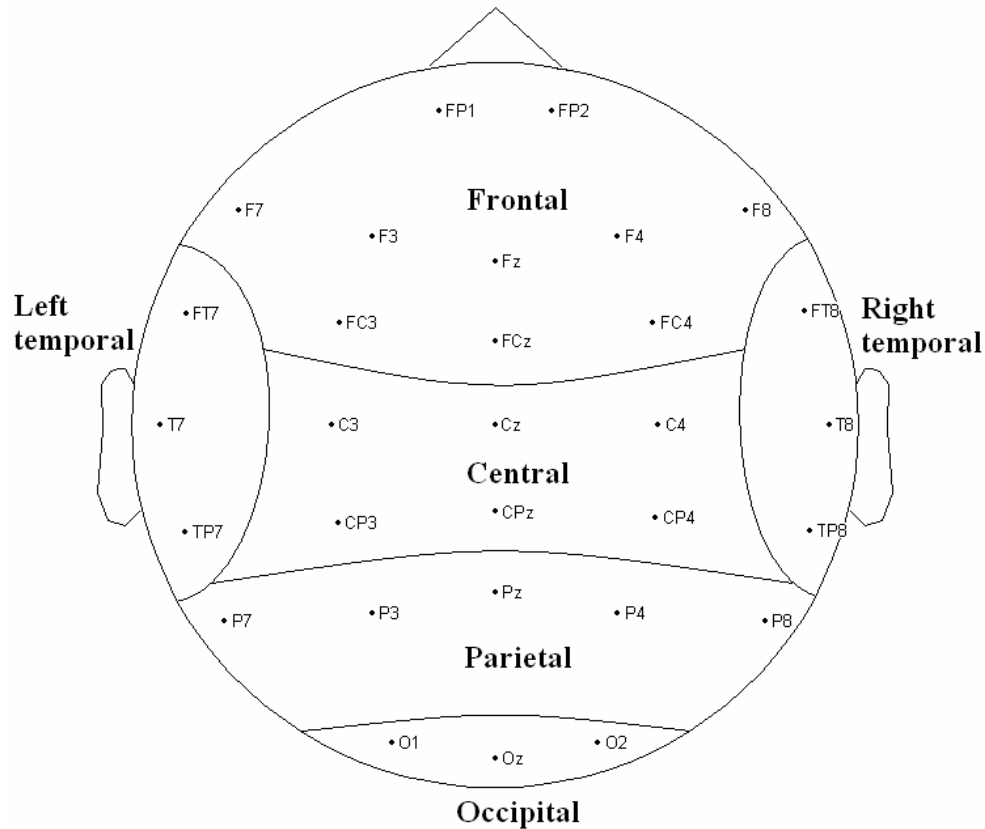


Figure 4-9: The locations of 30 recording electrodes and their respective region.

We calculated the ***incidence*** of each category based on a 2-minute frame. The window size was 2 seconds and no overlap between successive windows. Accordingly, ***incidence*** measures the probability of peak focalization at the same area based on 60's 2-sec epochs. The formula is shown below.

$$incidence = \frac{\text{Number of epoch belong to the category}}{\text{Total epochs in 2 - min (60 epochs)}} \qquad (4.6)$$

We laid more stress on the frontal, central and parietal areas where alpha

55

activities frequently appear. Figures 4-10 to 4-12 show the time-varying probabilities of source localization, respectively, in the frontal, central and parietal region of both groups. Beginnings of the main and the post session were marked by vertical dashed lines at the $2^{nd}$ and $32^{th}$ minute. The value at the $n^{th}$ minute was the group average of results analyzed for 10 subjects in each group, using the 2-min frame between $(n-1)^{th}$ and $(n+1)^{th}$ minute. For each category (area), *incidence* in the 2-min frame was compared with the pre-session result using *t-test* to evaluate the statistical significance of difference caused by meditation process. The asterisks on the top of the chart indicate the statistically significant difference ($p<0.05$) at those time points. For example, significant effect of meditation (relaxation) on frontal alpha was observed at the $25^{th}$ ($27^{th}$) minute for the experimental (control) group.
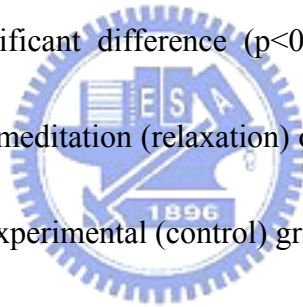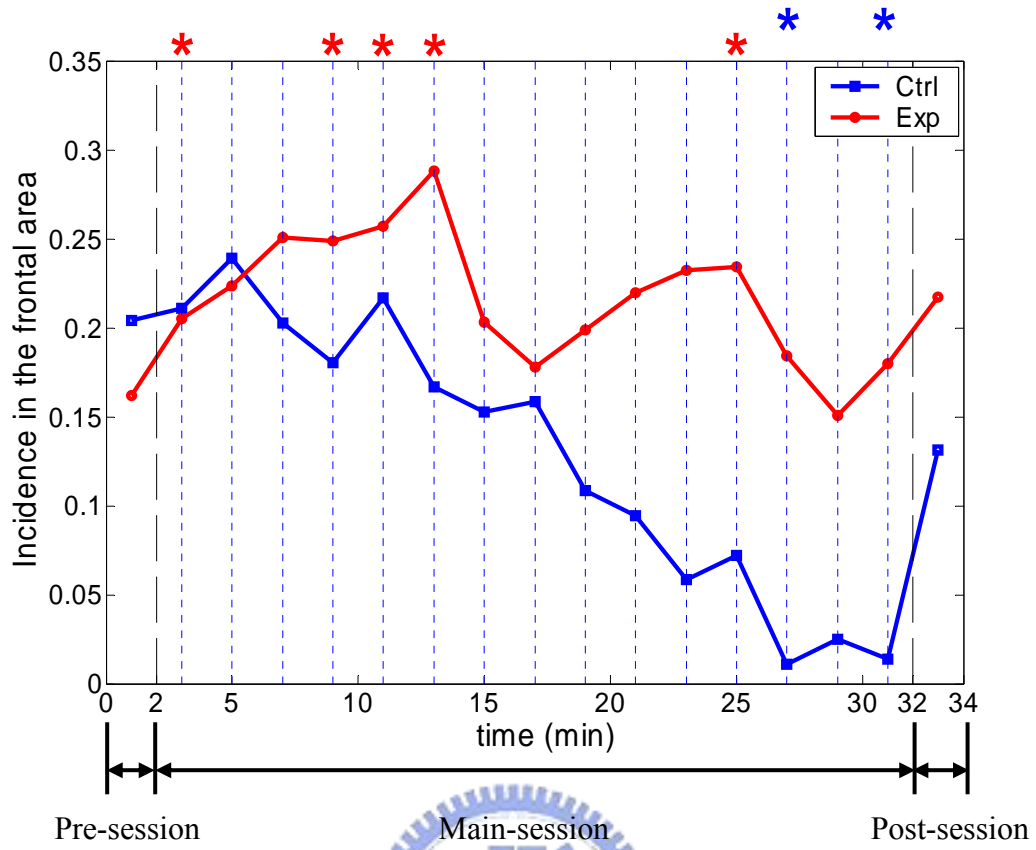
Figure 4-10: The incidence of frontal alpha of both groups.
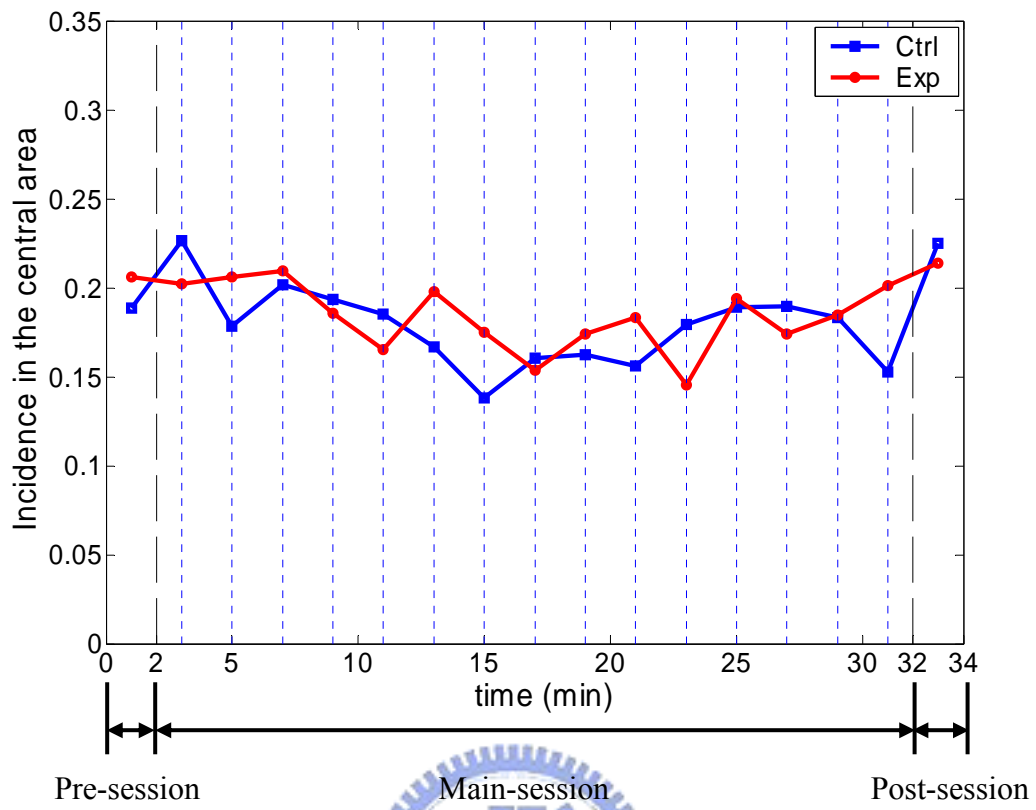
Figure 4-11: The incidence of central alpha of both groups.
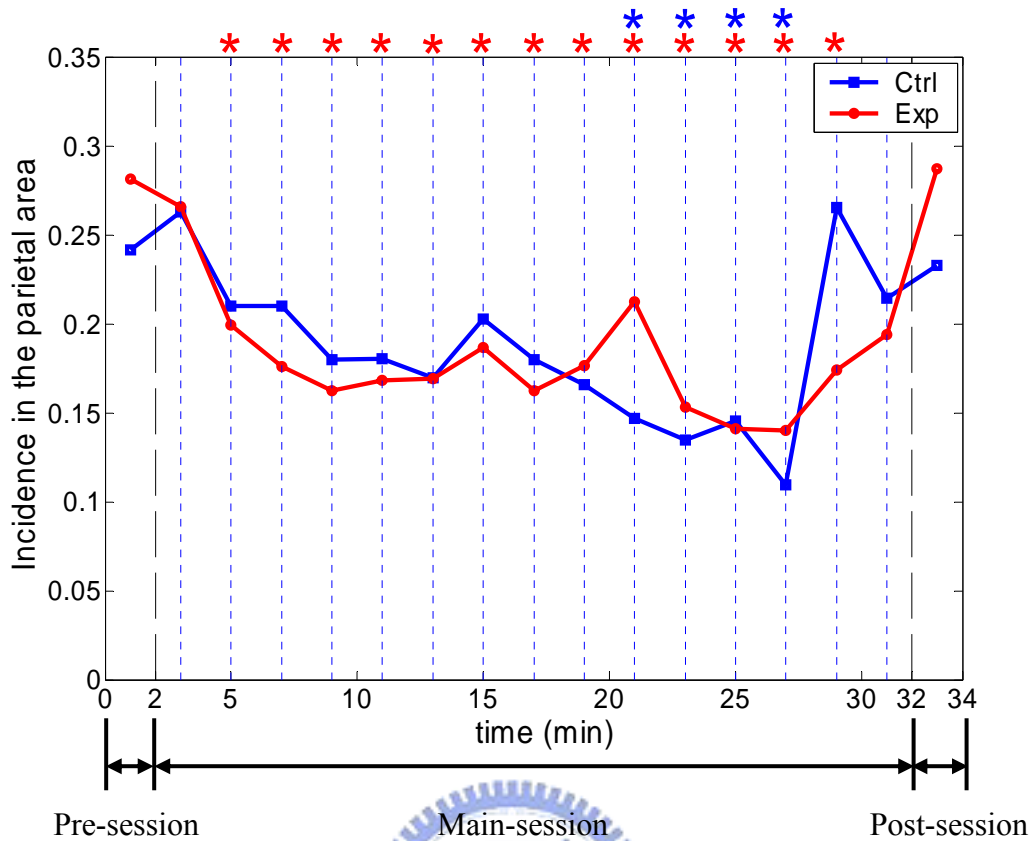
Figure 4-12: The incidence of parietal alpha of both groups.

Incidence of frontal alpha of the experimental group oscillates noticeably during

the entire recording session, as shown in Figure 4-10, with an increase in the early

meditation phase (3-13 minutes) followed by a dramatic drop afterwards (13-17

minutes). However, in the later phase of meditation the frontal alpha was increasing

again (17-25 minutes). On the other hand, control group exhibited quite different

results with decreasing frontal alpha in the entire main session. In addition,

statistically significant difference of frontal-alpha incidence between group averages

was observed by t-test ($p < 0.01$).

Figure 4-11 displays the group averages of incidence variations of central alpha.

Apparently, both curves show the similar trend for the entire recording session, that is, a slight reduction of central-alpha incidence during the main session following by an increase in the post session. As regards the spatio-temporal features of parietal alpha, incidence of the experimental group declined from the beginning of meditation and maintained till the end of meditation session (Figure 4-12). In the control group, the incidence presented a continuing decay in the whole relaxation session. Although these two groups showed similar trend, the consistency within each individual group was quite different. The experimental group revealed constant decrease in parietal alpha and showed significant difference at the early stage of meditation ($5^{th}$ minute), that was not observed in the control group until the $21^{th}$ minute of main session.

# Chapter 5

# Investigation of alpha-dependent F-VEPs under Zen meditation

Variation of brain dynamics under Zen meditation has been one of our major research interests for years. One issue encountered is the inaccessibility to the actual meditation level or stage as a reference. In this chapter, we propose an alternative strategy for investigating the human brain in response to external flash stimuli during Zen meditation course. To secure a consistent condition of the brain dynamics when applying stimulation, we designed a recording of flash visual evoked potentials (F-VEPs) based on a constant background EEG (electroencephalograph)–frontal $\alpha$-rhythm dominating activities that increase significantly during Zen meditation. Thus the flash-light stimulus was to be applied upon emergence of the frontal $\alpha$-rhythm. The alpha-dependent F-VEPs were then employed to inspect the effect of Zen meditation on brain dynamics. Based on the experimental protocol proposed, considerable differences between experimental and control groups were obtained.

## 5.1   Motivation of this research

Variations in EEG temporal and spatial activities have been presumed to be associated with the meditation stages, a comprehensive review was published recently (Cahn and Polich, 2006). Davison et al. found that long-term Buddhist practitioners self-induced sustained high-amplitude, gamma-band oscillations and phase-synchrony during meditation. These EEG patterns were noticeable especially at the lateral fronto-parietal electrodes (Davidson et al., 2003; Lutz et al., 2004). In Zen-meditation EEG study, increased alpha activity over the frontal regions of the brain has been observed during meditation (Kasamatsu and Hirai, 1966; Takahashi et al., 2005) and so has the increased frontal alpha coherence (Murata et al., 2004). Kasamatsu and Hirai found an increase in alpha amplitude at the beginning of meditation, which then spread frontally. Furthermore, Takahashi et al. observed that the increased frontal alpha power correlated with the enhancing internalized attention. Thus increased frontal alpha activity was hypothesized as a result of Zen-meditation process. All the observations have led into further understanding of the function-correlated, spatial characteristics of the brain affected by meditation. Another topic of interest in the meditation study involves the evoked potentials (EP) (or event-related potentials, ERP) under meditation. These studies include auditory evoked potential (AEP), somatosensory evoked potential (SEP), visual evoked potential (VEP), and so on.

Each parameter is meaningful to the respective perception function. Zhang et al. claimed that the amplitudes of F-VEPs (VEPs under flash stimuli) of Qigong meditators increased under meditation (Zhang et al., 1993). In Xu et al.'s research, the amplitude of F-VEP increased while the latency decreased (Xu et al., 1998). They suggested that concentration and attention may be the reason of altering the evoked potentials.

Due to unusual perceptions often experienced during meditation, human brain in response to external flash stimuli during Zen meditation draws our attention. Recording of VEPs provides a means of characterizing the visual pathway and visual function. VEPs can be recorded by applying either patterned or non-patterned stimulus that results in various VEP waveforms (Odom et al., 2004). Since practitioners must close their eyes during meditation, we employed non-patterned flashes in the VEP recording.

One problem encountered in the F-VEP study is to determine the appropriate timing for applying the flash-light stimulus. To our knowledge it has not been reported in regard to this issue. In our previous study, stimulus was applied at the mid-section of meditation at which subjects might undergo various physiological and mental states. In that case, F-VEPs were not able to reveal different experimental courses such as the section before, during, and after meditation (Liu and Lo, 2005). To

assure that all F-VEPs are acquired under a consistent condition, a rational experimental setup is to apply the stimulus based on a controllable factor. To gain access to particular brain states, one approach is to ask the subject to signal the attainment of the meditation state by finger movement (Lo et al., 2003; Takahashi et al., 2005; Newberg et al., 2001). However, it often causes meditators to break off from the meditation state.

To investigate the ERP activities in a given brain state defined by EEG, we thus conceive the idea of *EEG-triggered F-VEP* scheme, that is, the flash-light stimulus is applied under specific oscillatory features of the EEG. In this preliminary study, we intuitively select the frontal α-rhythm as the F-VEP triggered signal based on the previous results reviewed in this section and our empirical observations these years. The following section illustrates the methods for detecting the frontal α-rhythm and the experimental setup. Significant results obtained are discussed in the final section.

## 5.2 Systems and approach

According to the background description in the last section, the flash-light stimulus is to be applied upon emergence of the frontal α-rhythm. The scheme proposed in (Liao and Lo, 2006) is based on the autoregressive (AR) spectrum estimation. It provides more accurate estimate with better resolution (Hayes, 1996)

(Güler et al., 2001) and, in particular, allows on-line α-rhythm detection within a very small time frame. Modification of the scheme for on-line α-rhythm detection is described below.

### 5.2.1 Online α-rhythm detection

EEG signal is first decomposed into subband components by the tree structural filter bank, as shown in Fig. 5.1. According to Gabor's uncertainty principle (Oppenheim, 1998), downsampling operation improves frequency resolution which is desired for the

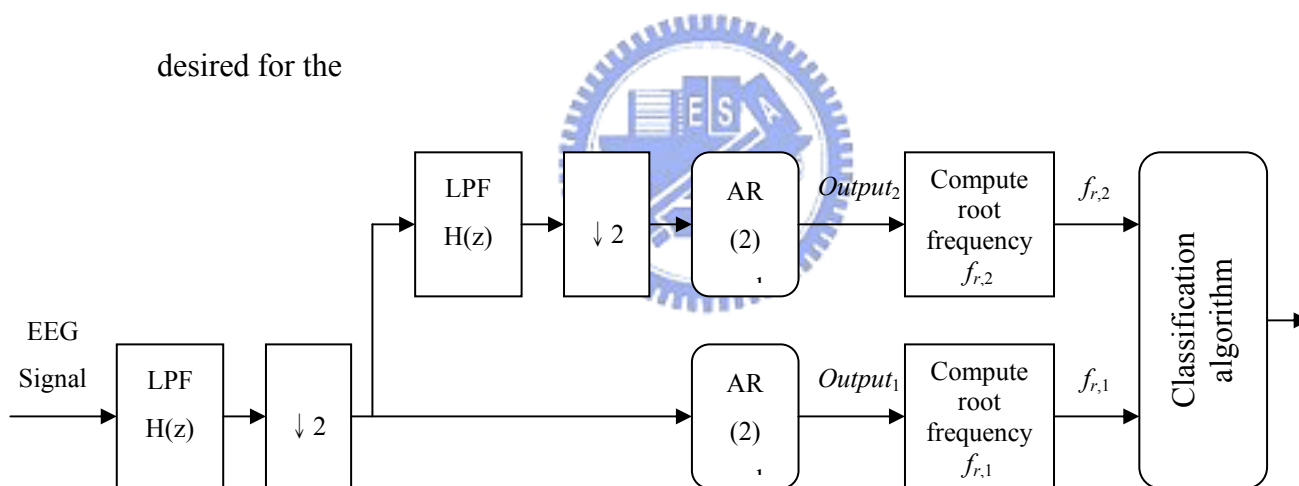

Fig. 5-1: Tree structural filter bank for the Subband-AR EEG Classifier. *H(z)* is

designed by least-squares error minimization with cutoff frequency 30Hz.

narrow-band EEG. Moreover, downsampling process makes the AR modeling better characterize the low frequency activities (Liao and Lo, 2006). We accordingly employ the subband-filtering scheme prior to the frequency analysis by AR modeling

for better frequency resolution and lower computation load. A linear-phase lowpass FIR filter $H(z)$ designed by using least-squares error minimization with cutoff frequency 30Hz is used as an anti-aliasing filter before the downsampling operation. Then the AR(2) model is applied to the decimated signal. Consider the EEG signal $x[n]$ generated by an autoregressive (AR(2)) process that is driven by the unit-variance white noise $w[n]$. An AR(2) model can be expressed as

$$x[n] + a_2[1]x[n-1] + a_2[2]x[n-2] = w[n]. \tag{5.1}$$

The model coefficients $a_2[k]$ can be determined by solving the autocorrelation normal equations (Hayes, 1996). After the model coefficients have been obtained, the conjugated pole pair is determined as,

$$-\frac{a_2[1]}{2} \pm j\frac{\sqrt{4a_2[2] - a_2{}^2[1]}}{2}. \tag{5.2}$$

Thus the root frequency of the signal can be obtained from Eq. (2)

$$f_{r,i} = \angle\left(-\frac{a_{2,i}[1]}{2} + j\frac{\sqrt{4a_{2,i}[2] - a_{2,i}{}^2[1]}}{2}\right) \tag{5.3}$$

where $i$ denotes the $i^{\text{th}}$ decomposition level. The filtering-and-downsampling process is reiterated to attain good accuracy in discriminating between α and δ/θ rhythms. The equivalent cutoff frequency is 15Hz. We design a criterion based on the root frequency to detect the α-rhythm. The algorithm examines each windowed segment to check whether it meets the following criterion.

*Criterion-*α: 7Hz<$f_{r,1}$<14Hz and 7Hz<$f_{r,2}$.

The root frequency $f_{r,1}$ is used to differentiate EEG rhythms in 0–14Hz from those in 14–30Hz. Next, root frequency $f_{r,2}$ is examined to screen out δ/θ rhythms.

Note that *output*$_1$ and *output*$_2$ are the results of downsampling (Fig. 5-1), the root frequency $f_{r,i}$ should be further divided by $2^i$. This experiment employs a window length of 1 second, with a moving step of 0.5 second.

## 5.2.2  Simulation

To verify the effectiveness of the α-rhythm detection algorithm, the algorithm is firstly applied to a simulated signal. We assume the sampling rate is 128Hz. The signal can be simulated by the pole placement method, that is, by placing each pole in the corresponding frequency band (Table 5-1) and adding Gaussian noise. As displayed in Fig. 5-2(e), the simulated 10-second signal is formed by connecting four segments of δ, θ, α, and β-rhythm patterns. Detection result in Fig. 5-2(e) is illustrated by two gray scales, with dark (light) gray indicating the α (non-α) pattern. The result clearly justifies the effectiveness of the algorithm in α detection.
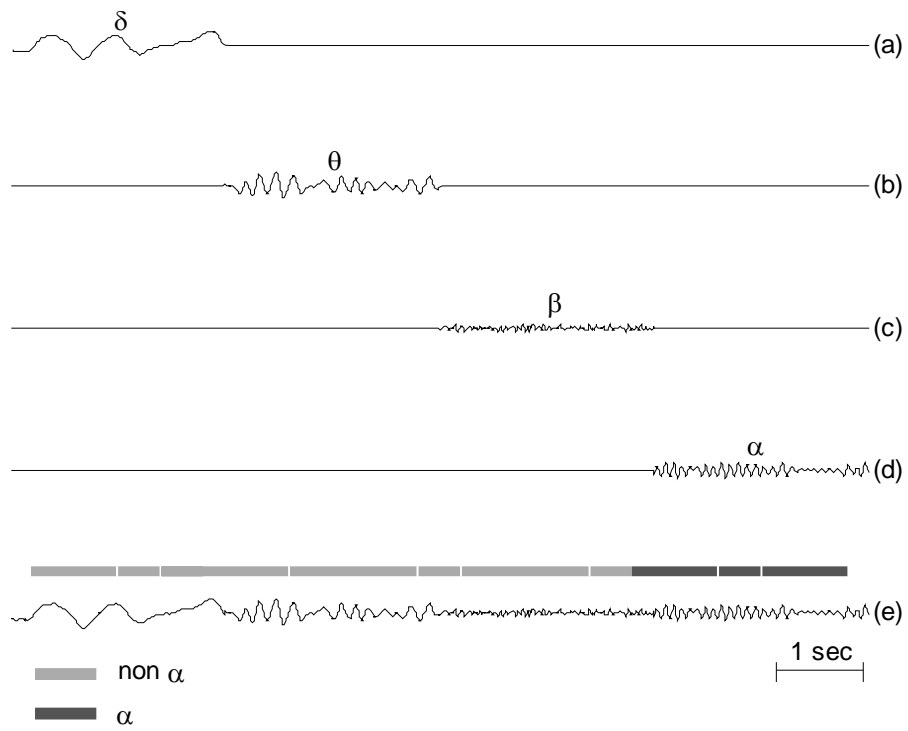
Fig. 5-2: Classification result of the simulated signal. Different grays are used to illustrated the $\alpha$ and non-$\alpha$ patterns.

Table 5-1: Locations of poles of the simulated signal

|  | Δ | θ | α | β |
|---|---|---|---|---|
| Poles' location | 0.98∠0.04 | 0.98∠0.16 | 0.98∠0.4 | 0.88∠0.63 |

### 5.2.3  Off-line alpha detection

Empirical EEGs often exhibit highly complex, irregular rhythmic patterns that make the recognition of specific EEG pattern more difficult. Our algorithm is robust in dealing with this kind of complication. Figure 5-3 displays the result of α detection. The error rate, estimated from the results of identifying 780 alpha candidates, was approximately 7.2% (4.6% false negative and 2.6% false positive rate) in comparison with the results of naked-eye examination by an experienced EEG interpreter.
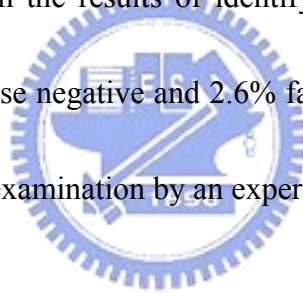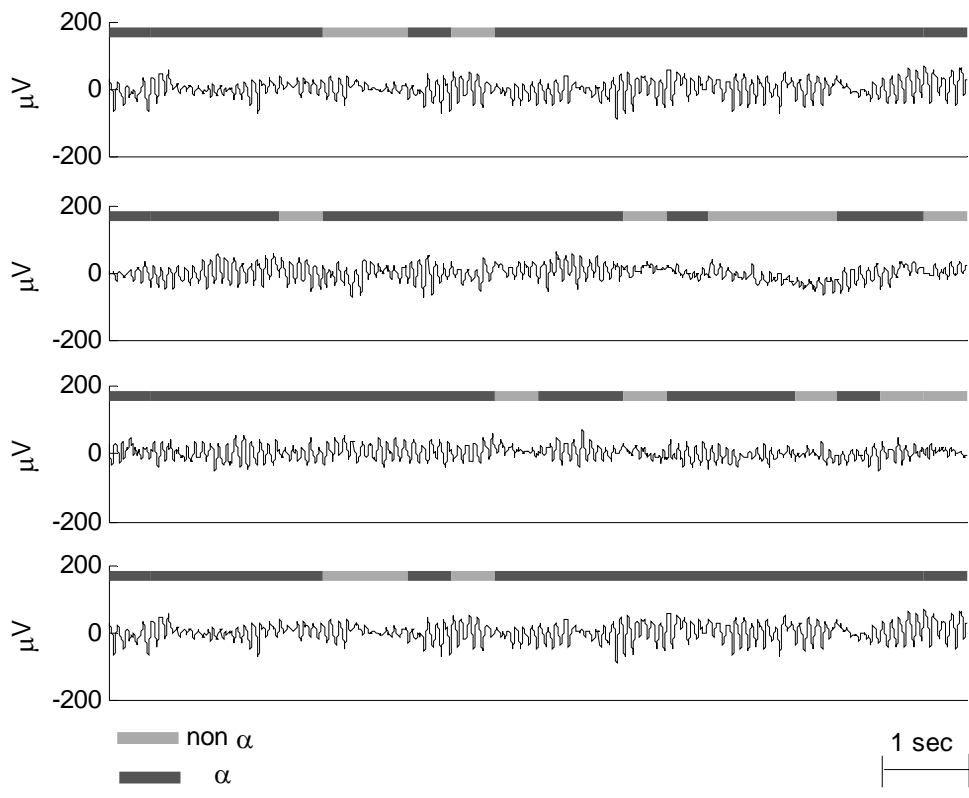
Fig. 5-3: Result of α detection for real EEG signal.

## 5.2.4 F-VEPs

The F-VEP consists of a series of negative and positive peaks, denoted respectively by N and P followed by a number. The number is referred to as the order (or time) of occurrence of that particular peak from the stimulus. The F-VEP source is located in the occipital lobe. Normally, the event-related brain potentials propagate via neural network toward the nearby regions. The phase differences among different channels are caused by the time delays of brain-wave propagation (Hughes et al., 1992). Figure 5-4 shows typical F-VEPs recorded on Fz, Cz, and Oz with corresponding peak labels. In this study, peaks of significance including N2, P2, N3, and P3 are to be analyzed. Note that F-VEPs of different channels have phase deviation.
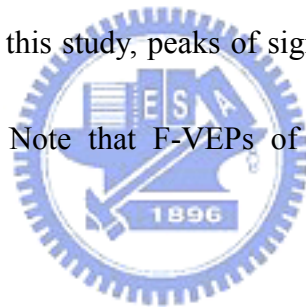
Researchers inferred that the noticeable negative peak N2 of Oz was generated in lamina IV cb (Kraut et al., 1985; Duccati et al., 1988), then the following positive peak P2 might reflect the inhibition activity within lamina. This study is mainly based on the hypothesis that Zen meditation affects visual neural pathway that can be revealed on the F-VEPs.
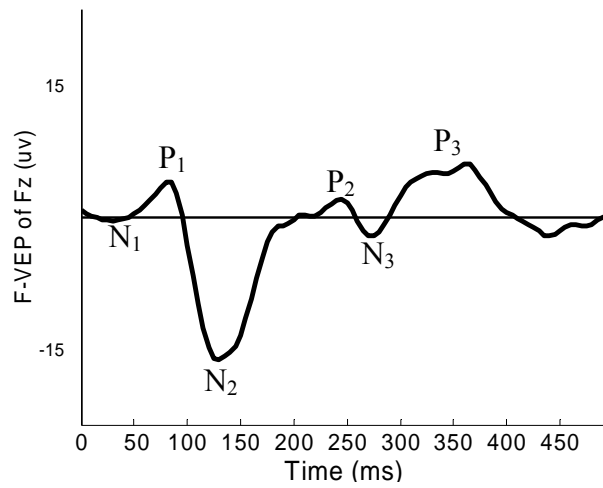
(a): F-VEP of Fz
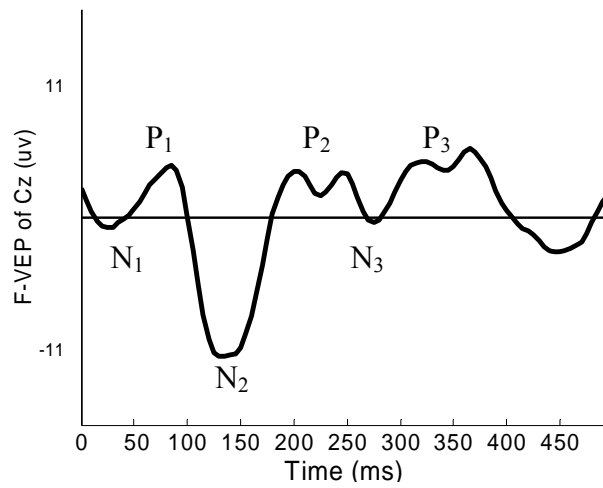


(b): F-VEP of Cz
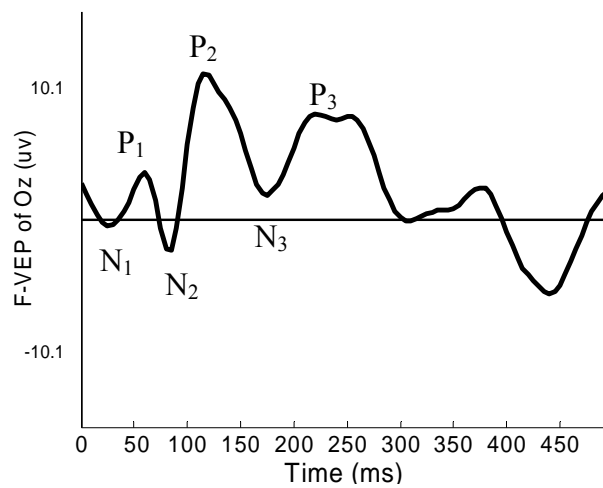


(c): F-VEP of Oz

Fig. 5-4: Profile of F-VEPs on (a) Fz, (b) Cz, and (c) Oz with corresponding peaks

labeled.

## 5.3 Experimental setup and protocol

### 5.3.1 Subjects

This study involves 11 meditators and 11 control subjects. In the experimental group, 4 females and 7 males at the mean age of $27.5 \pm 3.2$ years participated. Their experiences in Zen-Buddhist practice span $5.5 \pm 4.3$ years. The control group includes 3 female and 8 male students with an average age of $23.6 \pm 3.3$ years.

### 5.3.2 Apparatus

The EEG signals and F-VEPs were recorded at standard 10/20 positions with 32-channel SynAmps amplifiers (manufactured by NeuroScan, Inc.) connected to a Pentium-4 (1.5 GHz) PC. Common reference of linked MS1-MS2 (mastoid electrodes) was used. EEG signals, after amplification, were pre-filtered by a bandpass filter with passband 0.3–50 Hz, and digitized at 1000 Hz sampling rate. A 60-Hz digital notch filter was applied to the data to remove artifacts from power line or the surroundings.

We developed an online $\alpha$-detection algorithm that was implemented by using g.BSamp with g.RTsys (manufactured by Guger Technologies, Inc.) connected to a Pentium-M (1.4 MHz) notebook. g.BSamp is a stand-alone biosignal amplifier and g.RTsys is a biosignal acquisition and real-time analysis system for notebook implementation. To facilitate the real-time $\alpha$ detection, channel-Fz EEG was

pre-filtered by a bandpass filter with passband 0.5-30 Hz, and digitized at a lower rate

of 128 Hz. The α-detection algorithm was implemented on Simulink (MathWorks,

Inc., Natick, MA) with Real-Time Workshop. By generating real-time code with

Real-Time Workshop, the algorithm can be downloaded to the kernel and run in a

real-time manner under Windows (Guger et al., 2001). The experimental setup is

shown in Fig. 5-5. The subject stayed in an isolated space. A CCD camera positioned

in front of the subject was used to monitor the entire procedure. The 32-channel EEG

signals were recorded by an EEG recording system. Another computer read channel

Fz simultaneously to identify the occurrence of frontal-α rhythm. Once the frontal-α

was ascertained, the computer triggered the flash light controller to generate flash

stimuli.
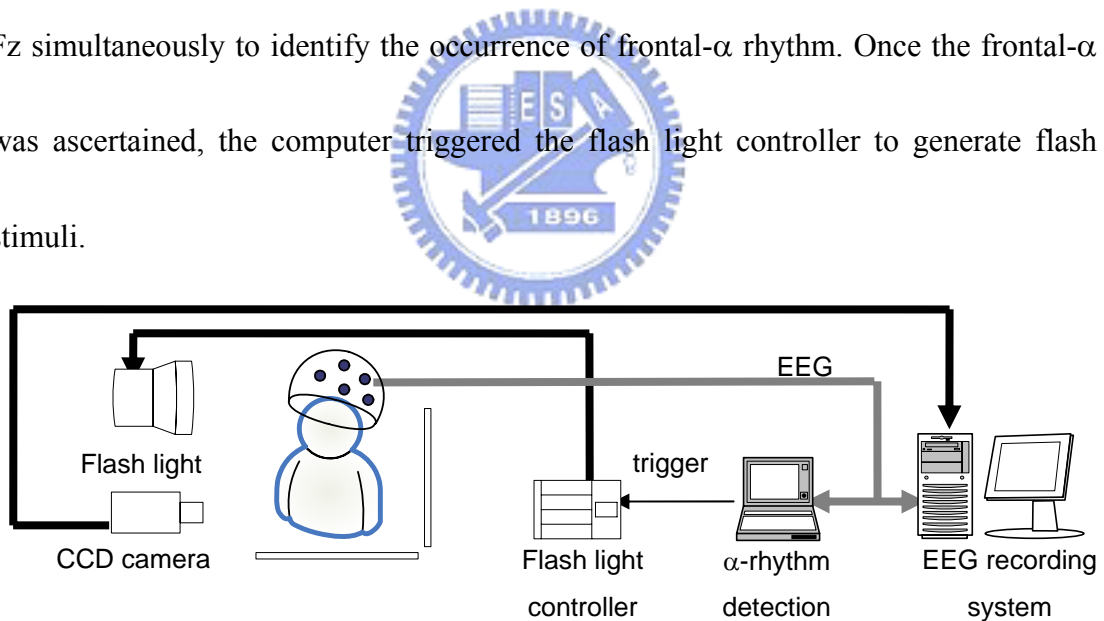


Fig. 5-5: Experimental setup for α-dependent F-VEP recording.

### 5.3.3　Experimental paradigms

During the experiment, subjects sat in a separated space in the laboratory. Each recording lasted for about 60 minutes, including three sections: two 10-minute background EEG recordings (section I and III) before and after a 40-minute recording (section II, the "main section") of EEG under meditation (experimental subject) or rest (control subject). The control subject sat in a normal, relaxed position with eyes closed, while the meditators practiced Zen-Buddhist meditation during the 40-minute main section. In Zen meditation, the subject sat, with eyes closed, in the full-lotus or half-lotus position. Each hand formed a special mudra (called the Grand Harmony Mudra), laid on the lap of the same side. The subject focused on the Zen Chakra and the Dharma Eye Chakra (also known as the "Third Eye Chakra") in the beginning of meditation till transcending the physical and mental realm. The Zen Chakra locates inside the third ventricle, while the Dharma Eye Chakra locates at the hypophysis (Lo et al., 2003).

The term "alpha-dependent F-VEPs" was used because we recorded F-VEPs upon the detection of frontal $\alpha$ rhythms. One run of alpha-dependent F-VEPs were recorded in each of the three sections (Fig. 5-6). Each run consisted of 50 alpha-dependent flash stimuli. The interval between two consecutive stimuli was longer than 1 sec. The flash light, with a 10μs duration, was produced by a xenon

lamp that was placed 60 cm in front of the subjects' eyes. Alpha-dependent F-VEPs were acquired from midline channels Oz, Cz and Fz, with the linked-mastoid electrode as the reference. Since we employed the mastoid-referenced unipolar montage, alpha activities could be found in the frontal channels of all subjects (Niedermeyer and Lopes da Silva, 2004). However, more frontal alpha activities were detected during meditation, that reduced the time required for collecting 50 alpha-dependent F-VEPs.
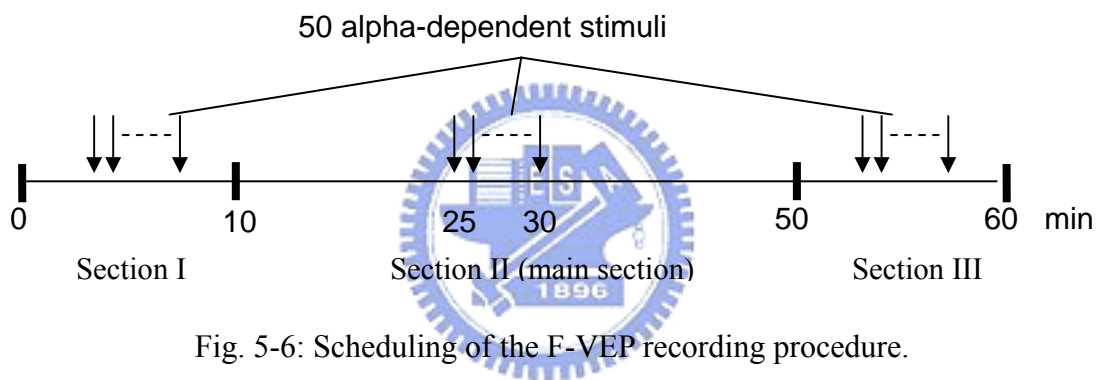


Fig. 5-6: Scheduling of the F-VEP recording procedure.

## 5.4 Results

As shown in Fig. 5-7, different codes were used to indicate the stimuli presented in different sections. The stimuli in section I, II, and III are marked by code 128, 64, and 32, respectively. And the marker at the upper left of each code indicates the time of flash stimulation. A concluding F-VEP of each section was derived by averaging 50 raw tracings in one run.
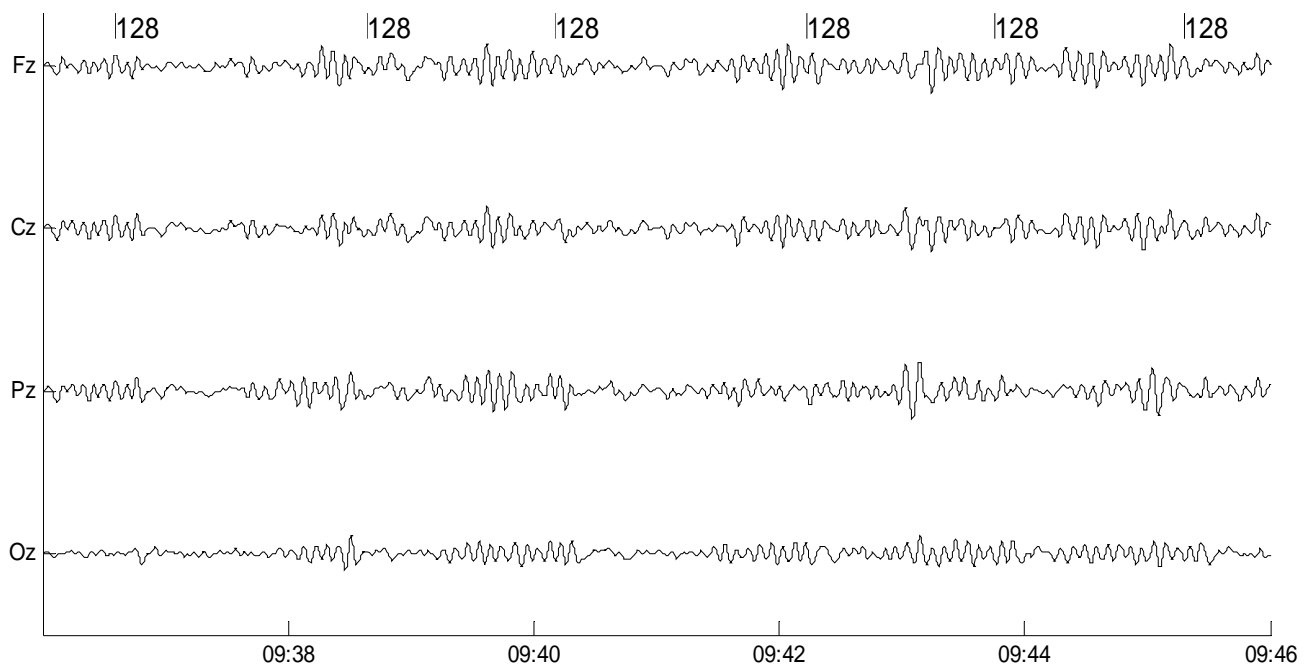


Fig. 5-7: Display format of selected channels (Fz, Cz, Pz, and Oz) for $\alpha$-dependent
F-VEP recording. The vertical bar at the upper left of mark '128' indicates the
time of applying flash stimulus.

Inter-subject variations of human VEP under the open experimental environment are complicated. We thus investigated the intra-subject differences among various

sections conducted in one experiment. We measured the amplitude and latency of the average F-VEP, and quantified the difference between various sections. Our results presented quite different trends between two groups. Figure 5-8 plots an example of the F-VEPs at Fz, Cz and Oz (from the top) for one subject. The solid lines represent the F-VEPs in the section I, and the dash and dot ones stand for those in the section II and III.

From our results we found that latencies of all components exhibit no significant difference among all sections in both groups. However, the variations of amplitudes show differences in some components between two groups. Table 5-2 presents, for each F-VEP component, ratios of the group average amplitudes of different sections. The p value is calculated by *paired t-test* (compared with selves in different phases) and *t-test* (compared to the other group in the same phase). Amplitudes of P1-N2 and N2-P2 on Cz and Fz increased significantly during meditation, yet, decreased during relaxation in the control group. On the other hand, N2-P2 amplitude on Fz decreased after meditation (experimental group) but increased after rest (control group). Apparently, the transit from one to another section caused F-VEP amplitudes on Cz and Fz to vary in opposite directions for both groups. We also observed significant differences between two groups in P1-N2 and N2-P2 amplitudes (Oz). P1-N2 amplitude (Oz) decreased during meditation but increased during rest. N2-P2

amplitude increased in the control group, but had little change in the experimental group. Contrary to the earlier peaks P1-N2 and N2-P2, N3-P3 amplitude (Oz) in the control group slightly decreased, whereas this peak amplitude increased in the experimental group.

Among all the F-VEP components, the most noticeable difference between two groups was the N2-P2 of Cz and Fz. Figure 5-9 plots the variations of N2-P2 amplitudes at Cz and Fz. Each bar represents the percentage of F-VEP varying from section I to section II $\left( \dfrac{II-I}{I} \times 100\% \right)$ for one subject (white: experimental subject, gray: control subject). Significant distinction is observed between two groups. Most meditation practitioners had their N2-P2 amplitudes increasing by an average rate of 20.1% (standard deviation among 11 subjects was 15.12%). Control subjects, on the contrary, exhibited a decreasing trend (average rate: −6.36%, standard deviation: 7.78%).
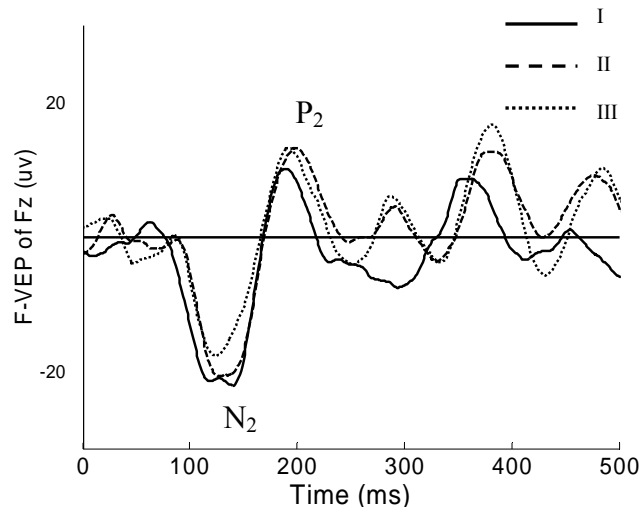
(a): F-VEP of Fz
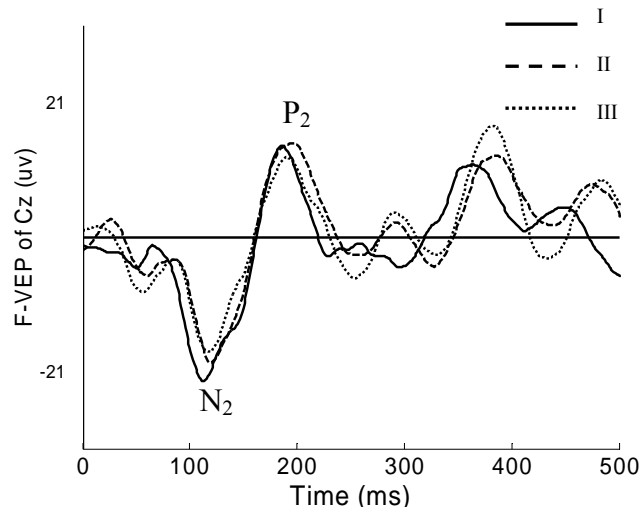


(b): F-VEP of Cz
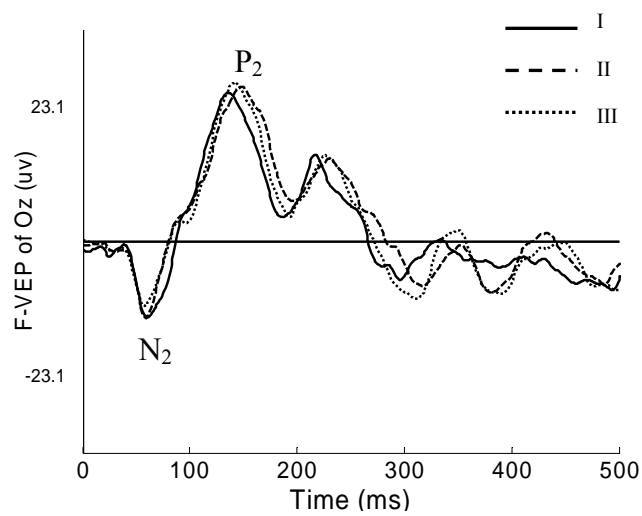


(c): F-VEP of Oz

Fig. 5-8: The α-dependent F-VEPs of one meditator recorded on (a) Fz, (b) Cz, and (c)

Oz.
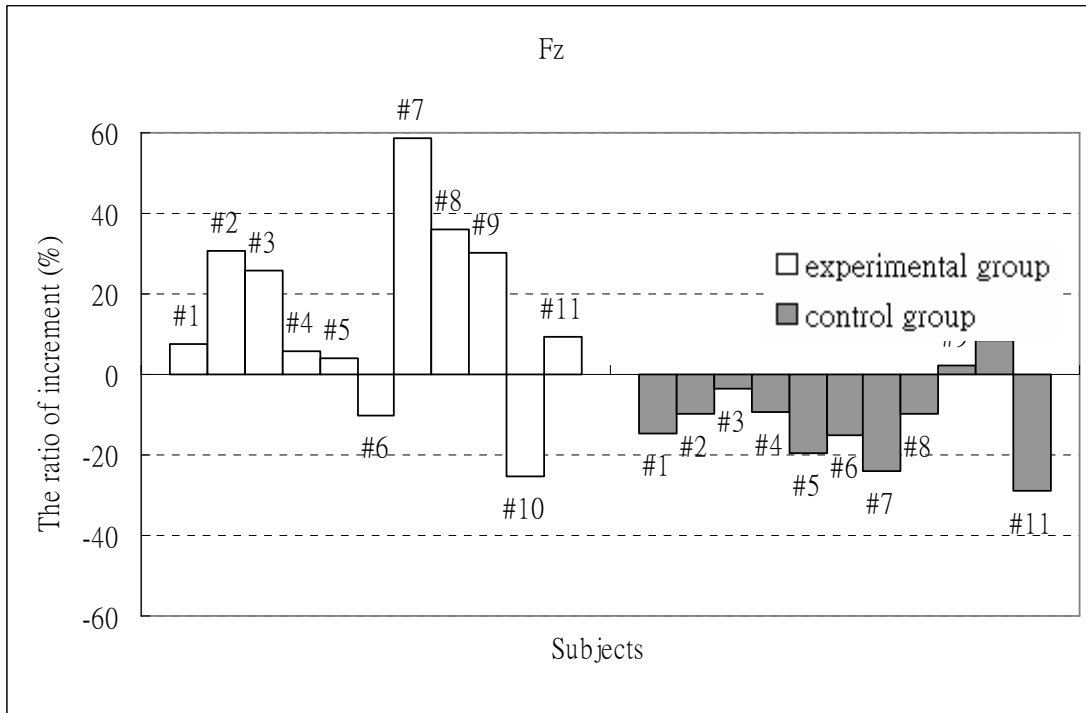
(a): Fz
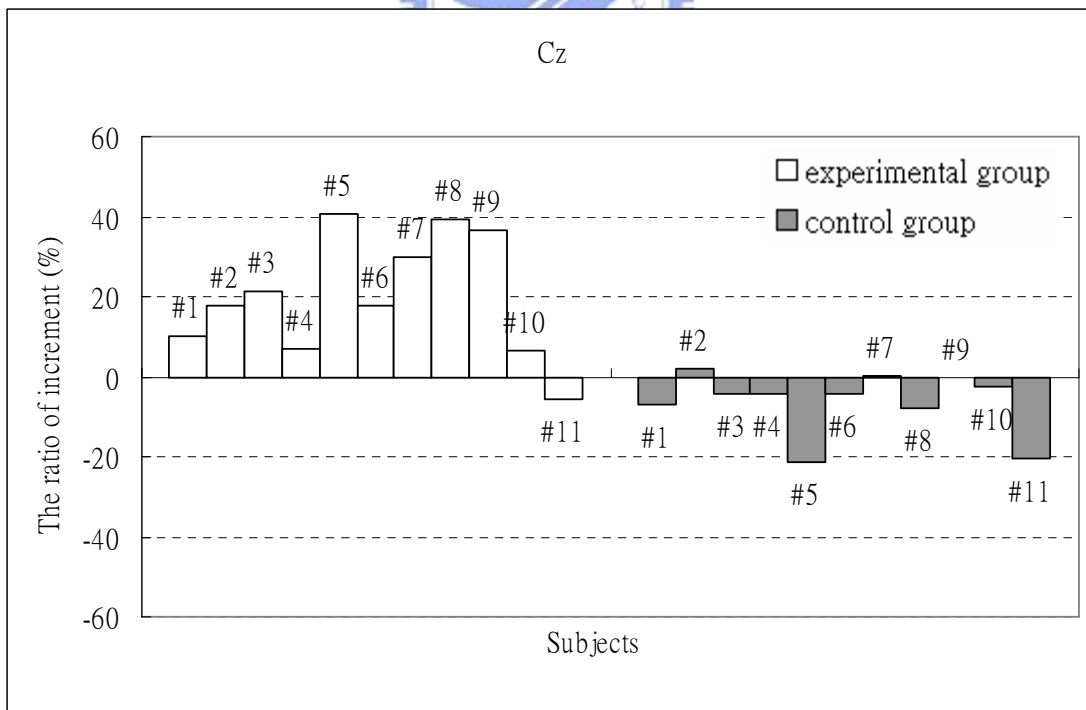


(b): Cz

Fig. 5-9: Variations of N2-P2 amplitudes at Cz and Fz. Each bar represents the

percentage of F-VEP varying from section I to section II $\left(\dfrac{\mathrm{II}-\mathrm{I}}{\mathrm{I}}\times100\%\right)$ for

each individual subject (white: experimental subject, gray: control subject).

Table 5-2: The changes in the peak amplitudes of specific F-VEP components.

| Item | | Exp group | | | Ctrl group | | | t-test | |
|---|---|---|---|---|---|---|---|---|---|
| | | II/I (%) | III/II (%) | P value (paired t-test) | II/I (%) | III/II (%) | P value (paired t-test) | II/I | III/II |
| Oz | P1-N2 | 95.09 | 114.40 | NS | 141.63 | 114.31 | NS | **0.013*** | NS |
| | N2-P2 | 101.41 | 101.44 | NS | 121.07 | 103.60 | NS | **0.010*** | NS |
| | P2-N3 | 107.10 | 102.77 | NS | 112.20 | 122.49 | NS | NS | NS |
| | N3-P3 | 117.33 | 106.86 | NS | 90.59 | 114.25 | NS | NS | NS |
| | P3-N4 | 121.35 | 104.18 | NS | 112.71 | 81.89 | NS | NS | **0.035*** |
| Cz | P1-N2 | 106.25 | 76.33 | **0.057** | 81.20 | 87.08 | NS | **0.043*** | NS |
| | N2-P2 | 120.10 | 89.18 | **0.00037*** | 93.64 | 102.01 | NS | **4.78E-05*** | NS |
| | P2-N3 | 134.73 | 103.43 | NS | 124.25 | 135.75 | NS | NS | NS |
| Fz | N1-P1 | 126.68 | 97.03 | NS | 104.30 | 125.79 | NS | NS | NS |
| | P1-N2 | 119.20 | 86.72 | **0.056** | 87.02 | 95.01 | NS | **0.043*** | NS |
| | N2-P2 | 115.70 | 92.76 | **0.040*** | 88.77 | 110.03 | **0.052** | **0.0025*** | **0.045*** |
| | P2-N3 | 143.35 | 128.01 | NS | 99.77 | 119.34 | NS | NS | NS |

I: section I, II: section II (main section), III: section III,

*: P<0.05,

NS: Not Significant

# Chapter 6

# Discussion and conclusion

## 6.1 Variation analysis of sphygmogram to assess the cardiovascular system under meditation

Why can Zen meditation improve the cardiovascular system? According to a number of researches and clinical reports, meditation practice has been proved to be effective in dealing with decreases of sympathetic nervous system tone, hypothalamic-pituitary-adrenocortical axis activation, and cortisol levels. Improvement of these functions has been associated with the improvement of cardiovascular system (Walton et al., 1995). In addition, meditation practice has been shown to reduce neurohormonal activities (Barnes et al., 2001) that might decrease shear stress on the circulatory system and further lighten the load on the heart.

During meditation, the meditation practitioners focus on their breathing, thus reducing dispersive thoughts, brain activity, muscle stress and the influence of the sympathetic system on blood vessels. Consequently, the artery wall may becomes more relaxed and elastic. In other words, the blood flow encounters less peripheral resistance and can more easily transport through organ, tissue, cell, etc. With a high

efficient circulatory system, human health improves.

Recently, complementary and alternative medicine (CAM) has driven researchers to investigate their scientific evidence. No doubt, meditation plays an important role in CAM. Here we report the immediate effect of Zen meditation on cardiovascular characteristics, with a control group involving the same number of normal, healthy subjects within the same age range. We analyzed the immediate effects because of the difficulty of controlling open-system experimental conditions for human subjects.

Diseases related to cardiovascular system have become the major death of the moderns. Meditation provides an alternative way of health care and maintenance. As a consequence, researchers are urged to develop scientific approach for exploring the underlying mechanism and the effects on body and mind. More scientific and clinical evidences may inject innovative ideas into mainstream medicine and popular healthcare practices. According to preliminary results of the BPW study, Zen meditation is more effective in improving cardiovascular characteristics than normal relaxation.

## 6.2 F-VEPs in meditation

In chapter 3, we have reported the differences of F-VEPs between the Zen-meditation practitioners and the normal healthy subjects. Latencies of the experimental group show no significant difference between sessions except P2 at site Oz. In Tsutsui's study [13], early latency components occurred before 70 msec, including P1-N2 at Oz and N1- P1 at Cz and Fz, whereas late latency components occurred after them (Tsutsui, 1987). At Oz, it was claimed that late latency components (P2~N4 at Oz in our data) originated from the cortex, and P2 was thought the inhibitory effect of lamina (Ducati et al., 1988; Givre, 1994). Accordingly, our results apparently reflect the substantial effects of Zen meditation on the cortex correlating with higher level brain function.

Two groups show the opposite variations in the amplitudes of late components, N3-P3 and P3-N4 at Oz, that indicates the suppression (enhancement) of the late-component responses via meditation (relaxation). The reason may be the influences of the background EEG. This observation further supports an alternative viewpoint of meditation that exhibits distinct effects on the brain nervous system in comparison with the normal relaxation.

Another significant distinction between two groups is the amplitude of P1-N2 at the fronto-central region (Cz and Fz). Note that P1 is the early component (generated

from the visual pathway and the primary visual cortex) and N2 is a late one. From the results of P1-N2, we may infer that meditation affects the visual pathway, primary visual cortex and the cortex, that the effects are different from those of relaxation.

In sum, meditation affects the late-latency components of the occipital F-VEP, yet, the earlier components of the fronto-central F-VEPs. One possible hypothesis states that the meditators concentrate their attention and inner energy on the Zen Chakra or Dharma Chakra, therefore neorons at the fronto-central regions become more active to enhance the visual evoked potentials from primary visual cortex and the association area. Further study is underway to provide firm evidence.
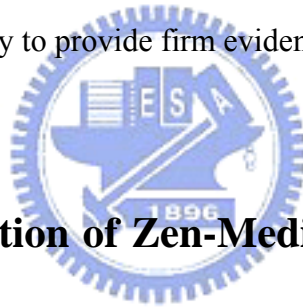
## 6.3 Spatial Focalization of Zen-Meditation Brain Based on EEG

In chapter 4, we developed a scheme to investigate the spatiotemporal behavior of alpha power in Zen-meditation practitioners. Consistent increase of frontal alpha in the beginning of meditation can be recognized as the major distinction between meditation and relaxation. At this stage of meditation, according to meditators' narration, they calmed down their mind and shut off their sensors to the outside stimuli by concentrating their attention on a specific chakra. Such inward attention conduct may result in the increase of frontal alpha (Aftanas and Golocheikine, 2001).

As meditation was underway, frontal alpha decreased notably that signified the possibility of consciousness transition to the state of awareness of the inner energy (Lo et al., 2003).

While practitioners entered the deep meditation stage, they often perceived inner light and had the blissful feelings, with the sense of time and space fading away (Alex, 2006). The frontal-alpha incidence increased in this state (about $17^{th} \sim 25^{th}$ minute). On the other hand, the attenuation of frontal alpha observed during last few minutes of meditation highly correlated with the fact that some practitioners returned to normal, attentive consciousness. Suppression of parietal alpha in both groups behaved quite the same. Nerberg et al. reported that the decreasing parietal alpha in meditators was caused by the state of mind more imperceptible to the external stimulus (Nerberg et al., 2001). Come control subjects fell drowsiness in the later half of relaxation session, causing the dropout of alpha activities (Niedermeyer and Lopez da Silva, 1999). Although both groups revealed decreasing parietal alpha, the mechanisms of modulating alpha are quite different.

To sum up, an important finding in this paper is the meditation states possibly inferred by alpha: mindful attention to reduce mental activities, transition to internal awareness, and "inner-light" perception, respectively, corresponding to the evolution of increasing → decreasing → increasing frontal alpha.

## 6.4 Investigation of visual perception under Zen Meditation based on alpha-dependent F-VEPs

In chapter 5, we have reported an alternative strategy to investigate the effects of Zen-meditation on human brain. Alpha-dependent F-VEP analysis was suggested as a standardized and consistent scheme for investigating the event-related response dependency on oscillatory features of the meditation EEG. Without any access into the real system dynamics of the brain, scientific study requires manipulating the experiment under pre-specified conditions. Accordingly, alpha-dependent F-VEPs were collected under the consistent alpha-dominating background EEG that increased significantly during Zen meditation process. Based on the same scheme, the online $\alpha$-detection algorithm could be modified for investigating the brain evoked response under given background EEG activity associated with other brain states, for example, theta- or beta-dominating background rhythms.

Our study has shown a great difference in the amplitudes of F-VEPs between the experimental and control group. Apparently, the meditation process modulates the amplitudes of F-VEPs under frontal $\alpha$-rhythm emergence, especially components P1-N2 and N2-P2. These three peaks P1, N2 and P2, emerge respectively at about 80, 120 and 190 ms after photic stimulation. Moreover, such F-VEP amplitude variations for Zen-meditation practitioners were more consistent at the electrode locus Cz than at

Fz. Since subjects mostly focused on the Zen Chakra (the third ventricle) during Zen meditation, we thus infer that meditation *focusing* changes the brain dynamics and the sensory responses to the external stimulus.

According to the literatures of visual function research, P1 component is generated from the major striate area, and N2 and P2 are generated from V4 which might be related to selective attention (Ducati et al., 1988) (Tsutsui, 1987; Skrandies, 1995). The increase of F-VEP amplitude indicates that Zen meditation, differing from normal relaxation, may cause some effects on primary visual cortex, central cortex, and frontal cortex. The study may assist in further understanding the intrinsic mechanism of such evidence as improving efficiency of the concept learning and integrating the brain function via Zen-meditation that has been reported.
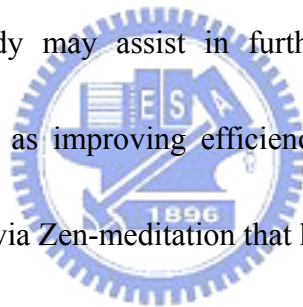
## 6.5   Discussion

In this dissertation, we investigated Zen meditation effects on cardiovascular system and CNS electrophysiological behaviors. BPW study demonstrates that meditation strengthened the elasticity and efficiency of blood vessels. According to the narrations of meditation practitioners, Qi energy circulates inside the body during meditation that may enhance blood circulation. This phenomenon "Qi leads blood" has been one of the major notions in traditional Chinese medicine since two thousand

years ago. Although the real mechanism of Qi is still unclear, our research has made a significant stride in the aspect of its physiological effect.

According to F-VEP study, meditation mainly imposed the effect in the late phase (about 250 to 350 mesc) on occipital site as well as in the early phase (about 70 to 150 msec) on central and frontal sites. Late phase of evoked potential was reported in neurophysiology to correlate to the visual pathway and cognition. According to the neurocognitive study, the late component at ~300 millisecond is normally larger while receiving an unexpected stimulus. In our results, F-VEP late components were smaller in meditation practitioners that might imply their lighter (more insensitive) response to the flash light.

On the other hand, would the frontal alpha emerging during meditation influence the F-VEP amplitude? This issue has been preliminarily studied in chapter 5. According to Lazar et al.'s study, brain regions associated with attention, including prefrontal cortex, were thicker in meditation practitioners than controls (Lazar et al., 2005). For this reason, emergence of alpha might imply the *coherent resonance* of cerebral neurons. As a result, deviation of neural activities would be smaller, leading to a larger response to the stimulus. This inference might provide a feasible interpretation for our observation of higher amplitude at the frontal sites during meditation.

## 6.6 Future work

Research in meditation is still in its infancy. Human body is a delicate and magnificent 'sensor' capable of perceiving subtle effects produced by meditation, to such a scale that even scientific technology falls far behind. One of the most important issues concerns the access to actual knowledge of meditation state. At current stage, we mainly rely on post-recording interview. Sophisticated experimental protocol is required to gain access to meditation state without interfering with the meditation course.

*Microstate* analysis provides a framework for relating the microscopic properties of small group of neurons to the macroscopic or bulk properties of larger cerebral region, therefore, explaining brain dynamics of Zen meditation in totally different and pioneering aspect at the microscopic level. Future research can be devoted to the analysis of Zen-meditation microstate.
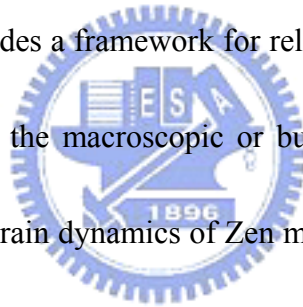
# Bibliography

Adrian ED and Mathews BHC, "The Berger rhythm: potential changes from the occipital lobes in man", *Brain*, vol. 57, pp.355-385, 1934

Aftanas LI and Golocheikine SA, "Human anterior and frontal midline theta and lower alpha reflect emotionally positive state and internalized attention: high-resolution EEG investigation of meditation", *Neuroscience Letters*, vol. 310, pp.57-60, 2001

Alex H., "Studies of Advanced Stages of Meditation in the Tibetan Buddhist and Vedic Traditions. I：A Comparison of General Changes," *Evidence-based Complementary and Alternative Medicine*, vol. 3, pp.513-521, 2006

Alexander CN, Schneider RH, Sheppard W, Clayborne BM, Rainforth M, Salerno J, Kondwani K, Smith S, Walton KG and Egan B. Trial of stress reduction for hypertension in older African Americans. *Hypertension,* vol. 28, pp.228-237, 1996

Andrew N, Abass A, Michael B, Michael P, Jill S and Eugene d'Aquili, "The measurement of regional cerebral blood flow during the complex cognitive task of meditation: a preliminary SPECT study," *Psychiatry Research: Neuroimaging Section*, vol. 106, pp.113-122, 2001

Banquet JP, "Spectral analysis of the EEG in meditation", *Electroenceph. Clin.*

*Neurophysiol.*, vol, 35, pp.143-151, 1973

Banquet JP, Lesèvre N, "Event-related potentials in altered states of consciousness",

*Prog. Brain Res.*, vol. 54, pp.447-453, 1980

Barnes VA, Treiber FA, Turner JR, Davis H and Strong WB, "Acute effects of

Transcendental Meditation on hemodynamic functioning in middle-aged adults,"

*Psychosom Med*, vol. 61, pp.525-531, 1999

Barnes VA, Treiber FA and Davis H, "Impact of Transcendental Meditation on

cardiovascular function at rest and during acute stress in adolescents with high

normal blood pressure," *J Psychosom Res*, vol. 51, pp.597-605, 2001

Barnes VA, Davis HC, Murzynowski JB and Treiber FA. Impact of meditation on

resting and ambulatory blood pressure and heart rate in youth. *Psychosom Med*,

vol. 66, pp.909-914, 2004

Basar E, Schurmann M, Basar-Eroglu C and Karakas S, "Alpha oscillations in brain

functioning: an integrative theory," *Int J Psychophysiol*, vol. 26, pp.5-29, 1997

Bezdek JC, *Fuzzy Mathemathics in Pattern Classification*. PhD Thesis,     Applied
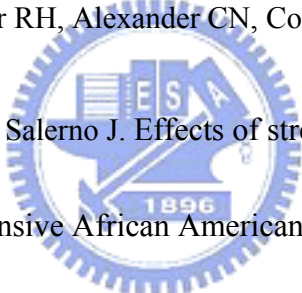
Math. Center, Cornell University, Ithaca, 1973

Cahn BR, Polich J, "Meditation States and Traits: EEG, ERP, and Neuroimaging

Studies", *Psychol. Bull.*, vol. 132, No. 2, pp.180-211, 2006

Cantero JL, Atienza M, Salas RM and Gómez CM, "Brain Spatial Microstates of

Human Spontaneous Alpha Activity in Relaxed Wakefulness, Drowsiness Period,

and REM Sleep," *Brain Topogr*, vol. 11, pp.257-263, 1999

Cantero JL, Atienza M, Gomez C and Salas RM, "Spectral structure and brain

mapping of human alpha activities in different arousal states,"

*Neuropsychobiology*, vol. 39, pp.110-116, 1999

Castillo-Richmond A, Schneider RH, Alexander CN, Cook R, Myers H, Nidich S,

Haney C, Rainforth M and Salerno J. Effects of stress reduction on carotid

atherosclerosis in hypertensive African Americans. *Stroke*, vol. 31, pp.568-573,

2000

Cigánek L, "The EEG response (evoked potential) to light stimulus in man",

*Electroencephalography and Clinical Neurophysiology,* vol. 13, pp.165-172,

1961

Cohn JN, Finkelstein S, Mcveigh G, Morgan D, Lemay L, Robinson J and Mock J.

Noninvasive pulse wave analysis for the early detection of vascular disease.

*Hypertension*, vol. 26, pp.503-508, 1995

Daubechies I, *Ten lectures on wavelets*. Philadelphia, PA: SIAM, 1992

Davidson RJ, Kabat-Zinn J, Schumacher J, Rosenkranz M, Muller D, Santorelli SF,
Urbanowski F, Harrington A, Bonus K, Sheridan JF, "Alterations in brain and
immune function produced by mindfulness meditation", *Psychosom. Med.*, vol.
65, pp.564-570, 2003

Dillbeck MC, Orme-Johnson DW, "Physiological differences between Transcendental
Meditation and rest," *Am Psychol.,* vol.42, pp. 879-881, 1987

Dragotti PL and Vetterli M, "Wavelet footprints: theory, algorithms, and applications,"
IEEE Trans. Signal Process., vol. 51, pp.1306-1323, 2003
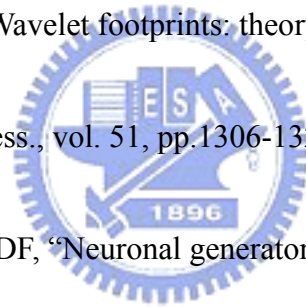
Ducati A, Fava E and Motti EDF, "Neuronal generators of visual evoked potentials:
intracerebral recording in awake humans", *Electroencephalography and Clinical
Neurophysiology,* vol. 71, pp.89-99, 1988

Ducati A, Fava E, Motti EDF, "Neuronal generators of visual evoked potentials:
intracerebral recording in awake humans", *Electroenceph. Clin. Neurophysiol.*,
vol. 71, pp.89-99, 1988

Elson BD, Hauri P, Cunis D, "Physiological changes in Yoga Meditation",
*Psychophysiology*, vol. 14, pp.52-57, 1977

Fey JF. *Contemporary Sphygmology in Traditional Chinese Medicine*. People's

Medical Publishing House, Beijing, 2003. (in Chinese)

Givre SJ, Schroeder CE and Arezzo JC, "Contribution of extrastriate area V4 to the

surface-recorded flash VEP in the awake macaque", *Vision Research*, vol. 34,

pp.415-428, 1994

Guger C, Schlögl A, Neuper C, Walterspacher D, Strein T, Pfurtscheller G, "Rapid

protyping of an EEG-Based Brain-computer Interface (BCI)", *IEEE Trans.

Neural. Syst. Rehabil. Eng.*, vol. 9, pp.49-58, 2001

Güler İ, Kiymik MK, Akin M, Alkan A, "AR spectral analysis of EEG signals by

using maximum likelihood estimation", *Comput. Biol. Med.*, vol. 31, pp.441-450,

2001

Han Y, Huan YW and Sun J. Spectral analysis of arterial pulse wave in patients with

hypertension. *Chinese Heart Journal*, vol. 12, pp. 178-192, 2000 (in Chinese)

Hankey A. Studies of Advanced Stages of Meditation in the Tibetan Buddhist and

Vedic Traditions. I: A Comparison of General Changes. *Evidence-based

Complementary and Alternative Medicine,* doi:10.1093/ecam/nel040, 2006

Hayes MH, *Statistical Digital Signal Processing and Modeling*. Canada: John Wiley

and Son, 1996

Hughes JR, Kuruvilla A, Fino JJ, "Topographic analysis of visual evoked potentials

from flash and pattern reversal stimuli: evidence for 'traveling waves'", *Brain

Topogr.*, vol. 4, pp.215-228, 1992

Jevning R, Wallace RK, Beidebach M, "The Physiology of Meditation: A review. A

Wakeful Hypometabolic Integrated Response", *Neurosci. Biobehav. Rev.*, vol. 16,

pp.415-424, 1992

Jones BM, "Changes in cytokine production in healthy subjects practicing Guolin

Qigong: A pilot study", *BMC Complement Altern Med,* vol. 1, pp. 8, 2001.

Kasamatsu A and Hirai T, "An electroencephalographic study on the Zen meditation

(Zazen)", *Folia Psychiatrica et Neurologica Japonica*, vol. 20, pp.315-336, 1966

Khir AW and Parker KH, "Measurements of wave speed and reflected waves in

elastic

tubes and bifurcations", *J Biomech* vol. 35, pp. 775-783, 2002

Kraut MA, Arezzo JC, Vaughan HG Jr, "Intracortical generators of the flash VEP in

monkeys", *Electroencephalogr. Clin. Neurophysiol.*, vol. 62, pp.300-312, 1985

Lazar SW, Kerr CE, Wasserman RH, Gray JR, Greve DN, Treadway MT, McGarvey

M, Quinn BT, Dusek JA, Benson H, Rauch SL, Moore CI, Fischl B, "Meditation

experience is associated with increased cortical thickness", *Neuroreport*, vol. 16, pp.1893-1897, 2005

Lehmann D, Brain electric microstates and cognition: the atoms of thought. In: E. R. John (Ed.), Machinery of the Mind. Birkhäuser, Boson, pp.209-224, 1990a

Liao HC and Lo PC, "Meditation EEG Overview Based on Subband Features Quantified by AR Model", *J. Intl. Soc. Life Info. Sci.*, vol. 24, pp.19-28, 2006

Lindberg DA, "Integrative Review of Research Related to Meditation, Spirituality, and the Elderly," *Geriatr Nurs*, vol. 26, pp. 372-377, 2005

Liu CY, Lo PC, "Flash Visual Evoked Potentials in Zen-Buddhist Meditation", *in 3$^{rd}$ Eur. Med. Biol. Eng. Conf.*, Prague, 2005.
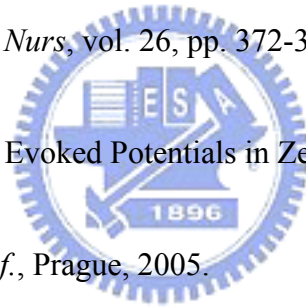
Lo PC, Huang ML, Chang KM, "EEG alpha blocking correlated with perception of inner light under Zen-Buddhism meditation", *Am. J. Chinese Med.*, vol. 31, pp.629-642, 2003

Lutz A, Greischar LL, Rawlings NB, Richard M, Davidson RJ, "Long-term meditators self-induce high-amplitude gamma synchrony during mental practice", *Proc. Natl. Acad. Sci. U.S.A.*, vol. 101, pp.16369-16373, 2004

McEvoy TM, Frumkin LR, and Harkins SW, "Effects of meditation on brainstem

auditory evoked potentials", *International Journal of Neuroscience*, vol. 10,

pp.165-170, 1980

Mcveigh GE, Bratteli CW, Morgan DJ, Alinder CM, Glasser SP, Finkelstein SM and

Cohn JN. Age-related abnormality in arterial compliance identified by pressure

contour analysis. *Hypertension*, vol. 33, pp.1392-1398, 1999

Milnor WR. *Hemodynamics*. Williams & Wilkins, Baltimore, 1989.

Murata T, Takahashi T, Hamada T, Omori M, Kosaka H, Yoshida H, Wada Y,

"Individual trait anxiety levels characterizing the properties of Zen meditation",

*Neuropsychobiology*, vol. 50, pp.189-194, 2004

National Center for Complementary and Alternative Medicine, "What is

Complementary and Alternative Medicine",

http://nccam.nih.gov/health/whatiscam/, 2002.

Newberg A, Alavi A, Baime M, Pourdehnad M, Santanna J, d'Aquili E, "The

measurement of regional cerebral blood flow during the complex cognitive task

of meditation: a preliminary SPECT study", *Psychiatry Res.: Neuroimaging

Section*, vol. 106, pp.113-122, 2001

Newberg AB and Iversen J, "The neural basis of the complex mental task of

meditation: neurotransmitter and neurochemical considerations," *Med Hypotheses,* vol. 61, pp.282-291, 2003

Nichols WW and O'Rourke MF. *McDonald's blood flow in arteries : theoretic, experimental, and clinical principles*. New York : Oxford University Press, 1998

Niedermeyer E and Lopes da Silva F, *Electroencephalography: basic principles, clinical applications and related fields*, Baltimore: Williams and Wilkins, 5th ed, pp.167-192, 2004

Odom JV, Bach M, Barber C, Brigell M, Marmor MF, Tormene AP, Holder G and Vaegan, "Visual evoked potentials standard", *Doc. Ophthalmol.*, *v*ol. 108, pp.115-123, 2004

Oppenheim AV, Schafer RW, Buck JR, *Discrete-Time Signal Processing*, New Jersey: Prentice Hall, 1998

O'Rourke1 MF, Pauca A and Jiang XJ, "Pulse wave analysis", *Br J Clin Pharmacol*, vol. 51, pp.507-522, 2001

Ott MJ, Norris RL and Bauer-Wu SM, "Mindfulness Meditation for Oncology Patients: A Discussion and Critical Review," *Integr Cancer Ther*, vol. 5, pp. 98-108, 2006

Schneider RH, Staggers F, Alexander CN, Sheppard W, Rainforth M,　Kondwani K,

Smith S and King CG, "A randomized controlled trial of stress reduction for hypertension in older African Americans", *Hypertension* vol. 26, pp.820-827, 1995

Shetty RC, "Meditation and its implications in nonpharmacological management of stress related emotions and cognitions," *Med Hypotheses*, vol. 65, pp. 1198-1199, 2005

Skrandies W, "Visual information processing: topography of brain electrical activity", *Biol. Psychol.*, vol. 40, pp.1-15, 1995

Takahashi T, Murata T, Hamada T, Omori M, Kosaka H, Kikuchi M, Yoshida H, Wada Y, "Changes in EEG and autonomic nervous activity during meditation and their association with personality traits", *Int. J. Psychophysiol.*, vol. 55, pp.199-207, 2005

Tan S, Tillisch K and Mayer E. Functional Somatic Syndromes: Emerging Biomedical Models and Traditional Chinese Medicine. *Evidence-based Complementary and Alternative Medicine*, vol. 1, pp.35-40, 2004

Telles S, Nagarathna R, Nagendra HR and Desiraju T, "Alterations in auditory middle latency evoked potentials during meditation on a meaningful symbol–"Om"", *International Journal of Neuroscience*, vol. 76, pp.87-93, 1994

Travis F, "Wallace RK. Autonomic and EEG patterns durin Eyes-Closed Rest and

Transcendental Meditation TM Practice: The Basis for a neural Model of TM

Practice", *Conscious Cogn.*, vol. 8, pp.302-318, 1999

Travis F, "Autonomic and EEG patterns distinguish transcending from other

experiences during Transcendental Meditation practice", *Int. J. Psychophysiol.*,

vol. 42, pp.1-9, 2001

Travis F, Tecce J, Arenander A and Wallace RK, "Patterns of EEG coherence, power,

and contingent negative variation characterize the integration of transcendental

and waking states," *Biol Psychol*, vol. 61, pp. 293-319, 2002

Tsutsui J, "Dynamic topography of the visual evoked potentials", *Rinsh Noha*,

vol. 29, pp.445-449, 1987 (in Japanese).

Wallace RK, "Physiological effects of transcendental meditation", *Science*, vol. 167,

pp.1751-1754, 1970

Wallace RK, H. Benson, A.F. Wilson, "A wakeful hypometabolic physiologic state",

*Am. J. Physiol.*, vol. 221, pp.795-799, 1971

Wallace RK, *Neurophysiology of Enlightenment*, Iowa: Maharishi University of

Management Press, 1986.

Walton KG, Pugh ND, Gelserloos P and Macrase P, "Stress reduction and preventing hypertension: preliminary support for a psychoneuroendocrine mechanism," *J Altern Complement Med*, vol. 1, pp. 263-283, 1995

West MA, "Meditation and the EEG", *Psychol. Med.*, Vol. 10, pp.369-375, 1980.

Wilkinson IB, Cockcroft JR and Webb DJ. Pulse wave analysis and arterial stiffness. *J Cardiovasc Pharmacol*, vol. 32, Suppl 3:S33-37, 1998

Woolfolk RL, "Psychophysiological correlates of meditation", *Arch. Gen. Psychiatry*, vol. 32, pp.1326-1333, 1975

Xie MZ, Li SZ and Li BX. Observation on ordinary person's parameter of pulse condition and pulse map. *Hunan Guiding Journal of TCMP*, vol. 6, pp.9-11, 2000 (in Chinese)

Xu M, Tomotake M, Ikuta T, Ishimoto Y and Okura M, "The effects of qi-gong and acupuncture on human cerebral evoked potentials and electroencephalogram", *The Journal of Medical Investigation*, vol. 44, pp.163-171, 1998

Xu M, Tomotake M, Ikuta T, Ishimoto Y and Okura M, "The effects of qi-gong and acupuncture on human cerebral evoked potentials and electroencephalogram", *J. Med. Invest.*, vol. 44, pp.163-171, 1998

Yamamoto S, Kitamura Y, Yamada N, Nakashima Y and Kuroda S, "Medial prefrontal

cortex and anterior cingulate cortex in the generation of alpha activity induced by

Transcendental Meditation: a magnetoencephalographic study," *Acta Med.*

*Okayama*, vol. 60, pp.51-58, 2006

Zhang W, Zheng R, Zhang B, Yu W, Shen X, "An observation of Flash Evoked

Cortical Potentials and qigong meditation", *Am. J. Chin. Med.*, vol. 21,

pp.243-249, 1993

# Appendix

The discrete wavelet transform (DWT) of a signal $x$ is calculated by passing it through a series of filters. First the samples are passed through a low pass filter with impulse response g resulting in a convolution of the two:

$$y[n] = (x * g)[n] = \sum_{k=-\infty}^{\infty} x[k]g[n-k]$$

The signal is also decomposed simultaneously using a high-pass filter $h$. The outputs giving the detail coefficients (from the high-pass filter) and approximation coefficients (from the low-pass). The two filters are related to each other and they are known as a quadrature mirror filter.

However, since half the frequencies of the signal have now been removed, half the samples can be discarded according to Nyquist's rule. The filter outputs are then downsampled by 2:

$$y_{low}[n] = \sum_{k=-\infty}^{\infty} x[k]g[2n-k]$$

$$y_{high}[n] = \sum_{k=-\infty}^{\infty} x[k]h[2n-k]$$

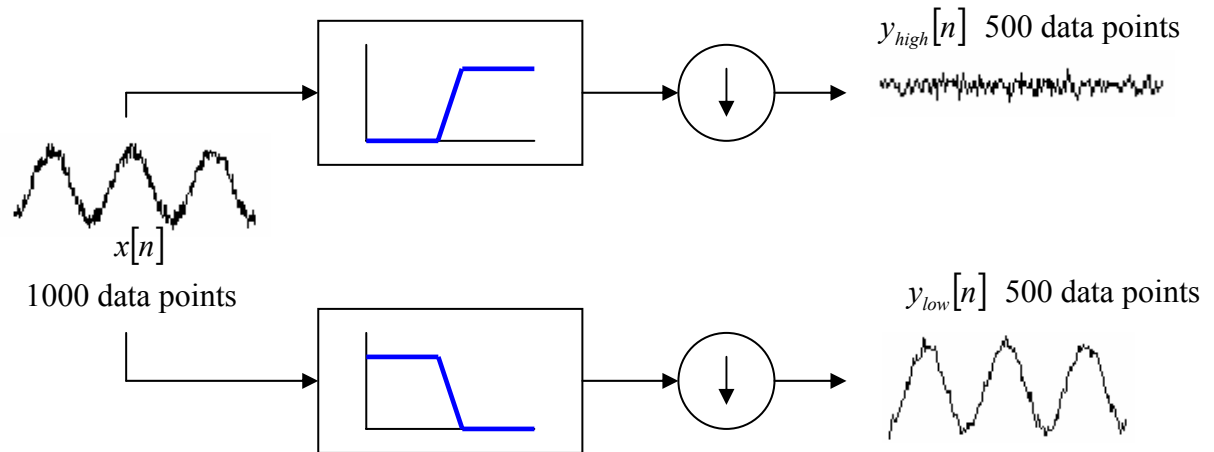Here is the schematic diagram with a real signal inserted into it.



Fig. A-1: The scheme diagram of the low-pass and high-pass filter

Here the output $y_{high}[n]$ is the high frequency DWT coefficients cD, and

$y_{low}[n]$ is the low frequency DWT coefficients cA. The decomposition process can be iterated, with successive approximations being decomposed in turn, so that one signal is broken down into many lower resolution components. This is called the *wavelet decomposition tree.* Below is the wavelet decomposition tree we used in chapter 5.
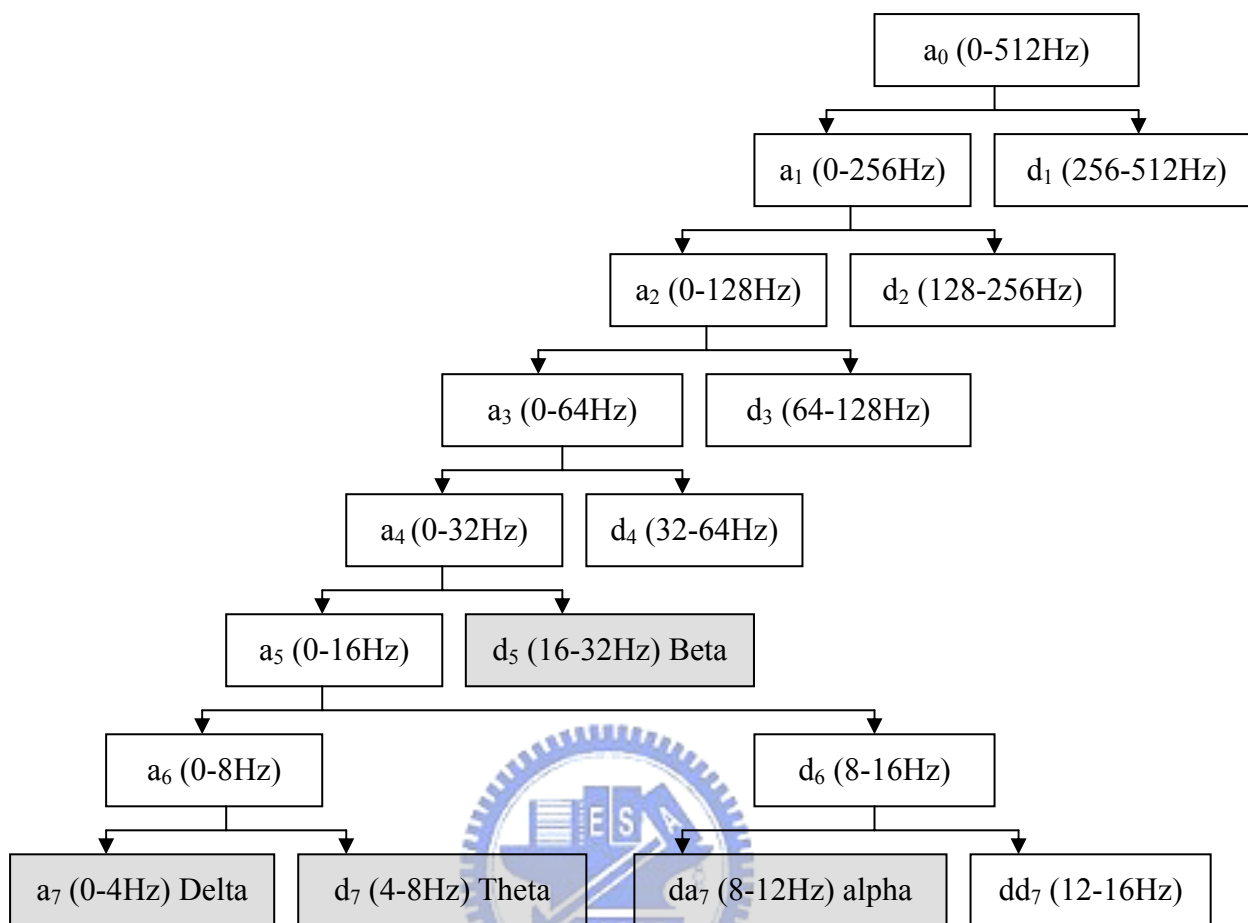
Fig. A-2: The wavelet decomposition tree

To calculate the power of each frequency band, we reconstruct the signal by assembling these coefficients back without any loss. Below is the process of decomposition and reconstruction
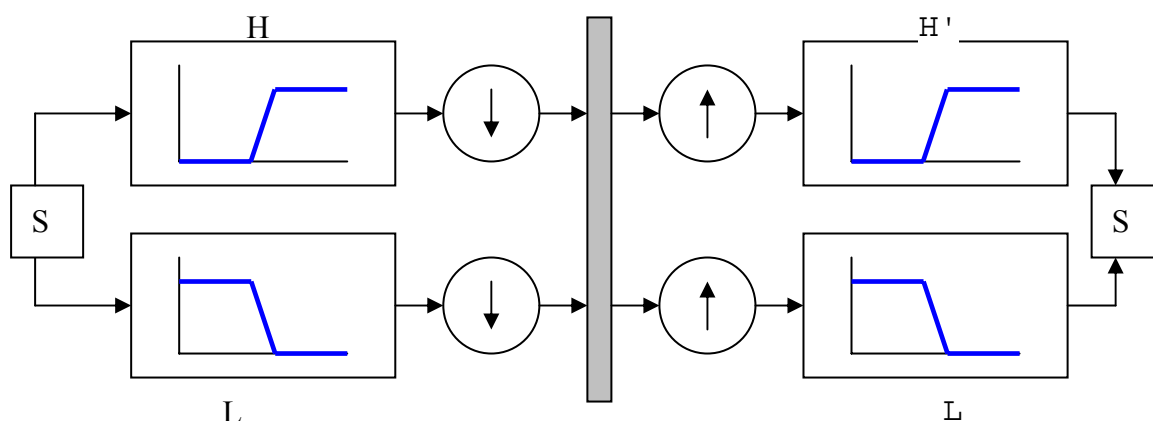


Fig. A-3: The process of decomposition and reconstruction

The low- and high-pass decomposition filters (`L` and `H`), together with their associated reconstruction filters (`L'` and `H'`), form a system of what is called *quadrature mirror filters*.

We pass the coefficient vector `cA1` through the same process we used to reconstruct the original signal. However, instead of combining it with the level-one detail `cD1`, we feed in a vector of zeros in place of the detail coefficients vector:
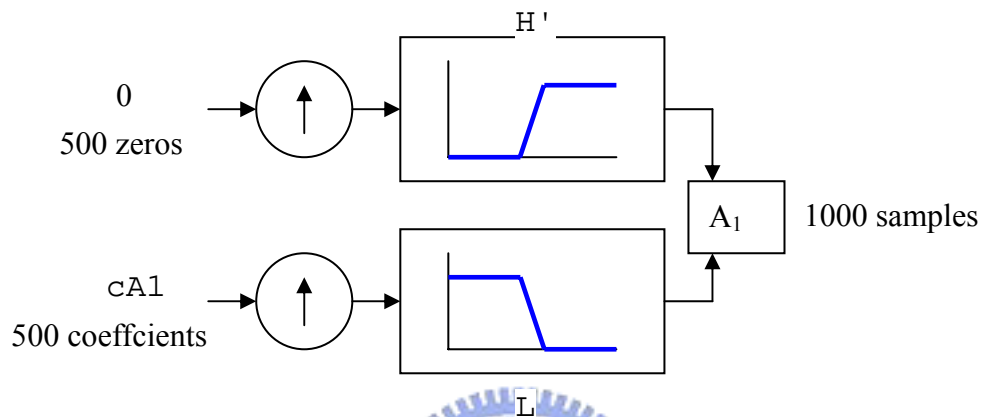


Fig. A-4: The process of reconstructing the low frequency component

The process yields a reconstructed *approximation* A1, which has the same length as the original signal S and which is a real approximation of it.

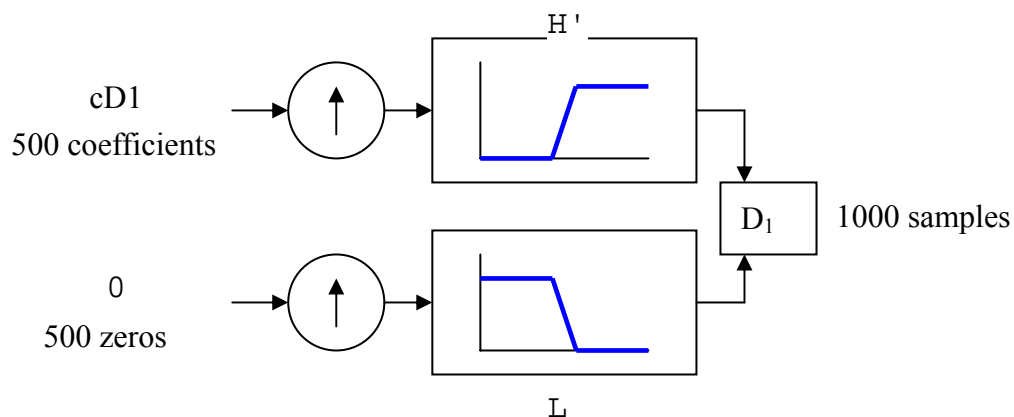Similarly, we can reconstruct the detail D1, using the analogous process:



Fig. A-5: The process of reconstructing the high frequency component

The reconstructed approximations and details are constituents of original signal. We utilize this method to reconstruct the level we are interested, and then calculate the power of it.

# Vita and Publication List

**Chuan-Yi Liu** received his B.C. degree in Electrical Engineering from National Taiwan University of Science and Technology, Taiwan in 1997 and Ph D. degree in Electrical and Control Engineering from National Chiao-Tung University, Taiwan in 2007. His research interests include biomedical signal processing, electrophysiological phenomenon, and pattern recognition and classification.

**Journal:**

1. CY Liu, CC Wei and PC Lo, "Variation Analysis of the Sphygmogram to Assess the Cardiovascular System under Meditation", *Evidence-based Complementary and Alternative Medicine* (Accepted)

2. HC Liao, CY Liu and PC Lo, "Investigation of Visual Perception under Zen-Meditation based on Alpha-dependent F-VEPs", *Journal of Biomedical Engineering Research,* Vol. 27, No. 6, pp. 384-391, 2006

3. CY Liu and PC Lo, "Spatial Focalization of Zen-Meditation Brain Based on EEG", *Journal of Biomedical Engineering Research* (Accepted)

4. CY Liu and PC Lo, "F-VEPs in Zen meditation", *Biomedical Engineering-Applications, Basis and Communications* (Accpted)

**Conference:**

1. Liu CY and Lo PC, "Flash-VEP in Meditation", International Symposium on Biomedical Engineering (ISOBME), Tainan, Taiwan, Dec 17-18, 2004

2. Chang KM, Liu CY and Lo PC, "An investigation of inner light during Zen meditation using alpha-suppressed EEG and VEP", 2nd International IEEE EMBS Conference on Neural Engineering, Washinton DC, USA. March 16-19, 2005, On page(s): 656- 659

3. Liu CY and Lo PC, "Flash Visual Evoked Potentials in Zen-Buddhist Meditation", 3rd European Medical & Biological Engineering Conference (EMBEC 2005), Prague (Czech Republic), Nov 20-25, 2005

4. Lin JD, <u>Liu CY</u> and Lo PC, "Evaluate the Effects of Meditation using Bioacoustic Vocal Profiling", International Symposium on Biomedical Engineering (ISOBME), Taipei, Taiwan, Dec 15-16, 2006

5. <u>Liu CY</u> and Lo PC, "Investigation of Spatial Characteristics of Meditation EEG Using Wavelet Analysis and Fuzzy Classifier", The 5th International Association of Science and Technology for Development (IASTED) Conference on Biomedical Engineering, Innsbruck, Austria, Feb 14-16, 2007